RADIO NOISE CHARACTERISTICS OF DIRECT CURRENT POINT-TO-PLANE CORONA

by

RODERICK SMIT MESECAR

A THESIS

submitted to

OREGON STATE COLLEGE

in partial fulfillment of
the requirements for the
degree of

MASTER OF SCIENCE

June 1958

APPROVED: [redacted]

Professor and Head of the Department of
Electrical Engineering

In Charge of Major

[redacted]

Chairman of School Graduate Committee

[redacted]

Dean of Graduate School

Date thesis is presented May 16, 1928

Typed by Phyllis Mesecar

ACKNOWLEDGMENTS

The work reported in this thesis was performed under the direction of L. N. Stone, Professor and Head of the Department of Electrical Engineering at Oregon State College. The author wishes to express his appreciation to Professor Stone for his many helpful suggestions, constructive criticisms, and advice.

It is a pleasure for the author to acknowledge the assistance of his wife, who typed the thesis.

TABLE OF CONTENTS

TABLE OF ILLUSTRATIONS

TABLE OF ILLUSTRATIONS (CONTINUED)

RADIO NOISE CHARACTERISTICS OF DIRECT CURRENT POINT-TO-PLANE CORONA

INTRODUCTION

The subject under investigation in this thesis is the radio noise generated by a point-to-plane corona current impulse source. The current impulses used were generated by a positive and a negative point-to-plane corona generator. It was found necessary to make a study of the operational characteristics of both types of corona generators because the corona from each differed considerably.

Measurement of radio noise generated by the corona current pulses was in conjunction with the National Electrical Manufacturers Association circuit for measuring radio noise. The corona current impulse generator was used as a reference radio noise generator for a comparison of input-output characteristics of the NEMA circuit. This was done to determine if the NEMA circuit altered the conducted radio noise.

APPARATUS USED IN THE STUDY OF DIRECT CURRENT POINT-TO-PLANE CORONA

Operational components of the corona generator and measuring equipment are shown in figure 1. The corona generator was constructed with two circular micarta ends, using eight steel rods for support. The generator shell was designed so that a glass cylinder could be placed inside the support rods to make a vacuum chamber. The plane electrode was made from a solid six-inch piece of stock aluminum. The front surface of the plane electrode was machined and highly polished. Supporting the plane is a sectional piece of aluminum which can be taken apart to obtain an eleven-inch variable gap. The last section of the support shaft is adjustable. The gap spacing is changed by turning the plane electrode.

The point was supported by two methods: First by a one-fourth inch aluminum shaft inserted into a small metal block and second, by an aluminum tube placed in a vee-shaped trough supported five inches above the micarta base on a pedestal.

Electrical connection to the point was made through a solid copper wire located about one inch above the micarta base. The copper wire terminates at the plug-in block, located at the edge of the base. The plug-in block has a switch for the selection of resistors. Ion-current was

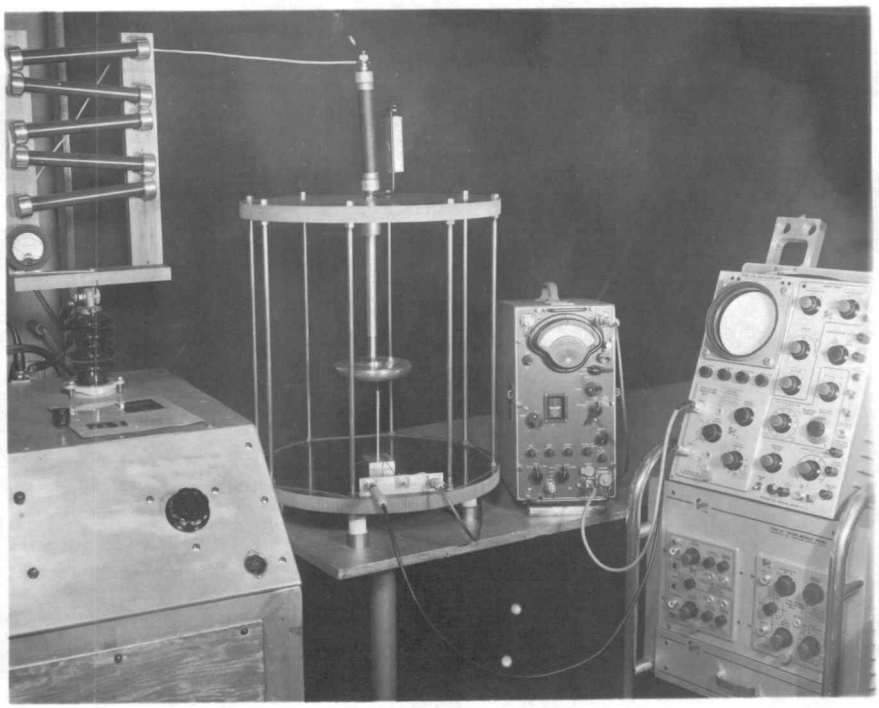

Figure 1

Apparatus used in the study of direct current point-to-plane radio noise characteristics.

L-R 20 kv d-c power supply
Corona generator
Stoddart radio-noise meter
(Model NM 20B)
Tektronix-type 535 oscilloscope

measured across a one-megohm resistor and pulse repetition periods are recorded across a 600-ohm resistor. Actually, the one-megohm resistor will not affect the repetition rate, but the RC-time constant of the one-megohm resistor and the coaxial cable capacitance will elongate the trailing edge of the pulse. The 600-ohm resistor is the recommended termination for the NEMA circuit.

Point-to-plane potential was supplied by a 20 kv direct-current power supply, shown in the left of the photograph in figure 1. A voltage-doubler circuit is used for the supply. The two output capacitors (one microfarad) are shunted with ten megohm resistors. This gives the power supply about a twenty-five second time constant. The use of this time constant is discussed later. Point-to-plane voltage was measured with five series connected four megohm (one-half percent) resistors, and an (0-1.0 ma) ammeter. The voltage is controlled by a variable transformer at the input to the voltage-doubler circuit.

A Tektronix-type 535 oscilloscope was used to record the output of the corona-current generator and the Stoddart Field Intensity instrument. The rise time of the type 53/54B vertical amplifier unit of the oscilloscope is 0.015 microseconds.

A Polaroid-Land camera was used to photograph the transient-wave forms displayed on the face of the oscilloscope cathode-ray tube.

The Stoddart (model NM 20-B) No. 188-8 Field Intensity meter was used to record the microvolts of radio noise generated by the current impulses. Input to the instrument was through the standard ten micro-microfarad capacitor. The Stoddart meter is a highly sensitive radio receiver operating as a selective radio-frequency voltmeter over the 150-kilocycle to 25-megacycle portion of the radio spectrum.

GENERATOR

The current impulse source used in the investigation was obtained by using the circuit schematically shown in figure 2. As indicated in the circuit, the generator consists of a variable high voltage direct-current supply and a point-to-plane electrode. Excluding the instrumentation, this circuit configuration constitutes a corona generator.

In 1938, the first study, in detail, of the corona generator was initiated by G. W. Trichel (5) and interpreted by L. B. Loeb. Trichel's study started with the investigation of a negative point-to-plane corona generator. A second study of positive-point corona (6) was made later.

The generator can produce positive and negative corona depending upon the polarity of the point; however, the characteristics of the types of corona differ considerably. In the course of this investigation, it became necessary to study both types. This study was made to obtain a better understanding of the generator characteristics with alterations in the point-to-plane configuration.

The characteristics of the positive point corona generator will be introduced first, and the negative point second.

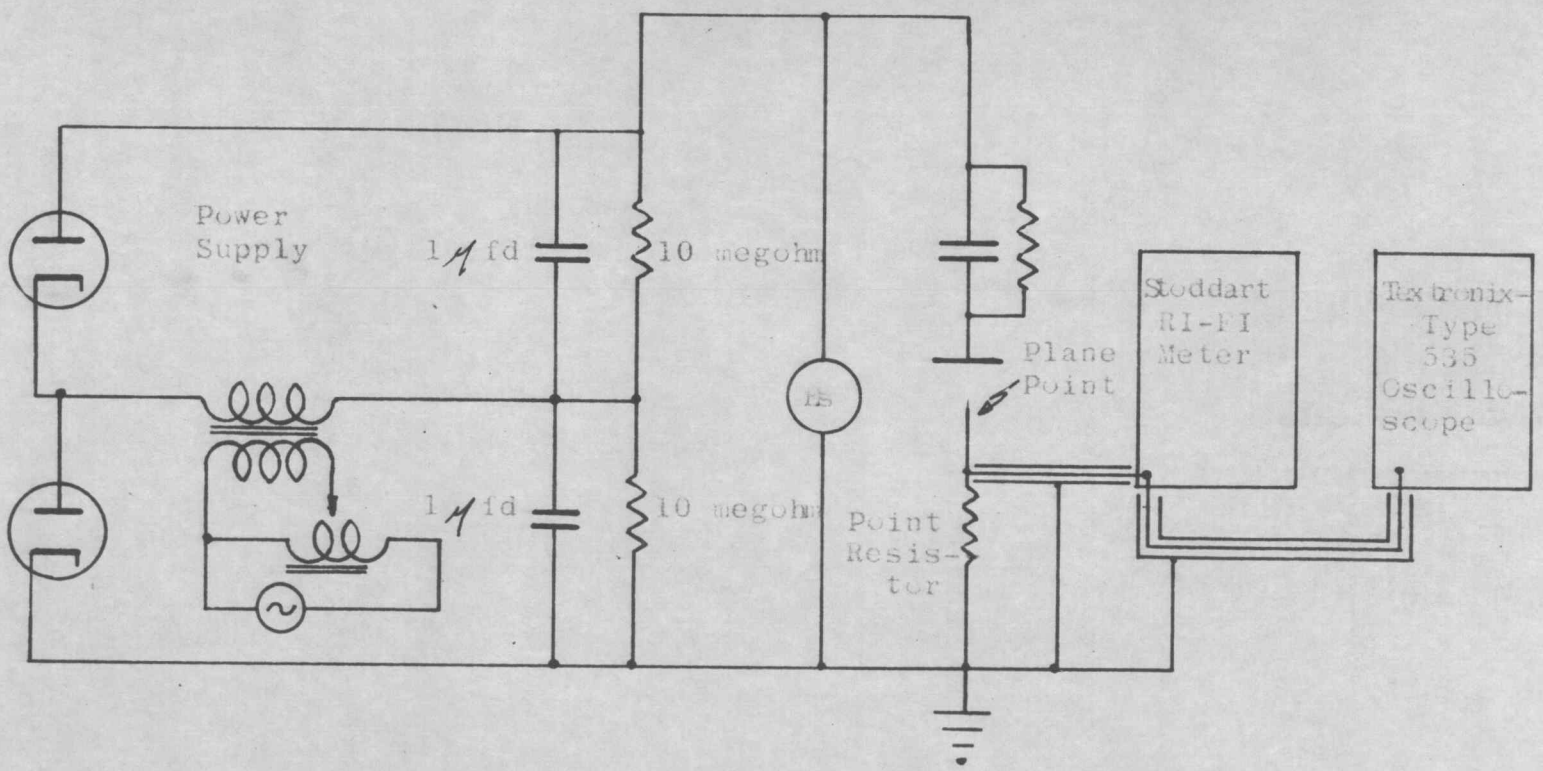

Figure 2. Schematic diagram of point-to-plane corona generator.

THEORY POSITIVE POINT CORONA IMPULSES

The first results of G. W. Trichel's study of positive point-to-plane corona (6) showed the ion-current pulses were "bursts" or "streamers". Both "bursts" and "streamers" are characterized by greater ionization than that possible by a single inrush of electrons to the positive point. The greater ionization is obtained by successive small avalanches which propagate a positive ion column toward the negative plane electrode. The mechanism operates in the following manner: The field at the point is increased to a critical value where electrons falling into the positive point will generate an electron avalanche by collision. Molecules losing these electrons form a positive ion column, which extends out from the point toward the plane. Ultraviolet light, produced during the initial electron avalanche, meanwhile produces more electrons by photoelectric ionization and makes new avalanches as the electrons fall into the intensified field of the extended point. This process repeats until the lower fields far out in the gap cause the self-propagation to stop. When the self-propagation has stopped, a relaxation time is necessary before another "burst" or "streamer" can propagate from the point. The relaxation time is dependent upon the time to restore the high fields about the point. The time for this high field

restoration can be altered by changing the field about the point. Essentially, the generator becomes a current-pulsing device with regular time intervals between pulses.

POSITIVE POINT CORONA GENERATOR

Initial studies of the positive point-to-plane corona generator were made to determine the generator's parameters so that it could be used as a current pulse source. The investigation started with the insertion of tungsten points, (appendix I) with hemispherical tips, into the rounded end of a one-fourth inch aluminum rod which acts as the point support. The points were elevated far enough above the rod to essentially be called unshielded. It was found difficult to obtain the positive corona without flashover on points with radii near 0.0108 inches and a 0.75 inch point-to-plane spacing.

When the point radius was decreased to 0.00337 inches, it was possible to maintain positive corona; however, the point-to-plane potential beyond onset was limited to three to four kilovolts increase before flashover. The pulse repetition frequency for this point was about 20 kilopulses per second. The allowable change in point-to-plane voltage did not permit an appreciable change in pulse repetition frequency.

Use of the small radii points over a short period of time would soon alter the point enough to change the generator's pulse characteristics. On occasions, after the generator had been functioning for five to ten minutes, it would suddenly flashover from point to plane. This ruined the point. Consequently, it was impossible to determine if it was deterioration of the point which caused the flashover. In any event, the very small radii points and small gap made the generator a sensitive unit to work with. A new point tip would begin to discolor, as though it had been heated, immediately after corona onset. The discoloration was more pronounced and extended further down on the smaller radii points.

Figure 3 is a multiple photograph to illustrate the increasing pulse height with increased point-to-plane potential. The left-hand pulse was photographed at a particular point voltage and then the point voltage was increased and the oscilloscope trace was moved horizontally to the position of the second pulse. This was done four times to show the series of pulse height changes that occurred over a two kilovolt change in potential beyond onset. A plot of the pulse height versus supply voltage (figure 5) results in an exponential function with a positive slope.

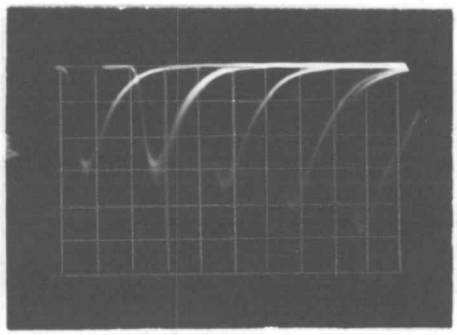

Figure 3. A multiple exposure showing the increasing pulse height with increasing positive point-to-plane voltage. (Left-right, Es = 7, 8,9,10,11 kv. Time - 0.1 μsec/cm voltage - 0.5 v/cm.)

Figure 4a. A positive point-to-plane current pulse. (Time - 0.01 μsec/cm voltage - 0.5 v/cm)

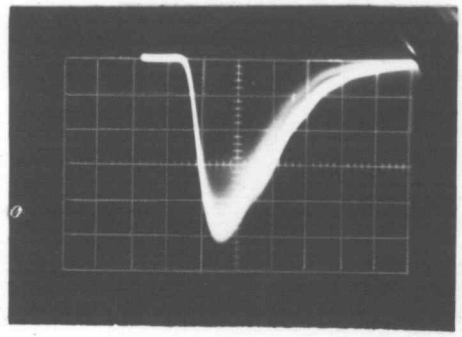

Figure 4b. This shows the positive point pulse repetition period. (Reference trace removed. Time - 100 μsec/cm.)

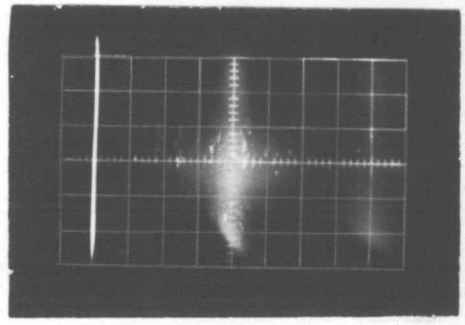

Figure 5

POSITIVE POINT-TO-PLANE
PULSE HEIGHT

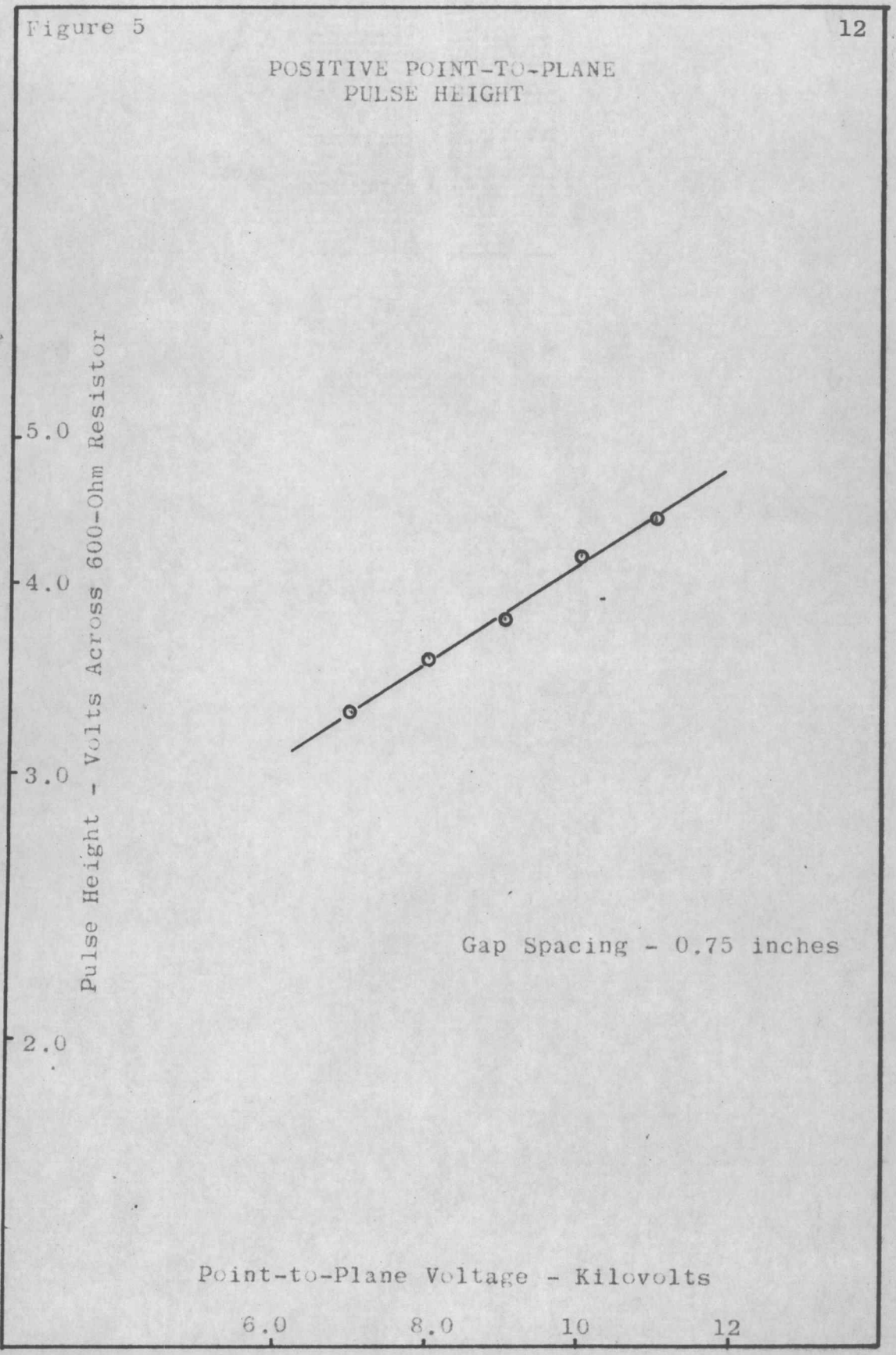

A different type of positive point-to-plane corona was achieved by semi-shielding a point on a tube. The corona produced in this case had a definite audible high-pitched whistle. This was quite different than the noiseless unshielded point corona. The blue-orange corona spire was visibly seen extending some distance into the gap. This type of corona mechanism would continue for a period of time without flashover.

Tubes ranging from 0.5 inches in diameter to 2.25 inches were used to evaluate the generator's pulsing characteristics. A vee-shaped trough was constructed on an aluminum pedestal to support the tubes. A small hole was drilled in the tube just the diameter of the point and a threaded device was added from the back of the tube to control point elevation. For the tube diameters used, the best point elevation was 3/32 of an inch. The point radius (0.00337 inches) was held constant for all tubes.

With a particular tube diameter and gap spacing, it was difficult to increase the point-to-plane potential without suffering a flashover. It was noticed, however, that just beyond the onset potential, the generator developed pulses with regular time intervals. This essentially meant that to obtain different pulse repetition rates, tube diameters and gap spacings had to be adjustable parameters. This resulted in an awkward method

of changing the repetition rate. Adjustment of the gap spacing required decreasing the supply voltage to zero and manually raising or lowering the plane electrode the proper distance.

Repetition rates encountered with the positive generator pulses are described in figure 6. The repetition rates were visually observed on a Tektronix-type 535 oscilloscope placed across a 600-ohm resistor in the point-to-ground circuit. The repetition frequency range of this point-tube generator configuration is between 2-10 kilopulses per second. Figure 4-a,b illustrates the positive-point pulse and the regular-spaced pulses. It was necessary to remove the oscilloscope reference trace in figure 4-b so that its light intensity would not obliterate the pulse trace. The first pulse is sharply defined because the oscilloscope is triggered by it. The second pulse is a discrete band which is caused by a small variation in relaxation time. This band can be narrowed if the point-to-plane potential establishes a high clearing field around the point. With a high clearing field, the ion-space charge is removed at more definite time intervals. Flashover will occur before the band is the width of a single pulse.

Figure 6

PULSE REPETITION FREQUENCY FOR
POSITIVE POINT ON TUBE TO PLANE
CORONA GENERATOR

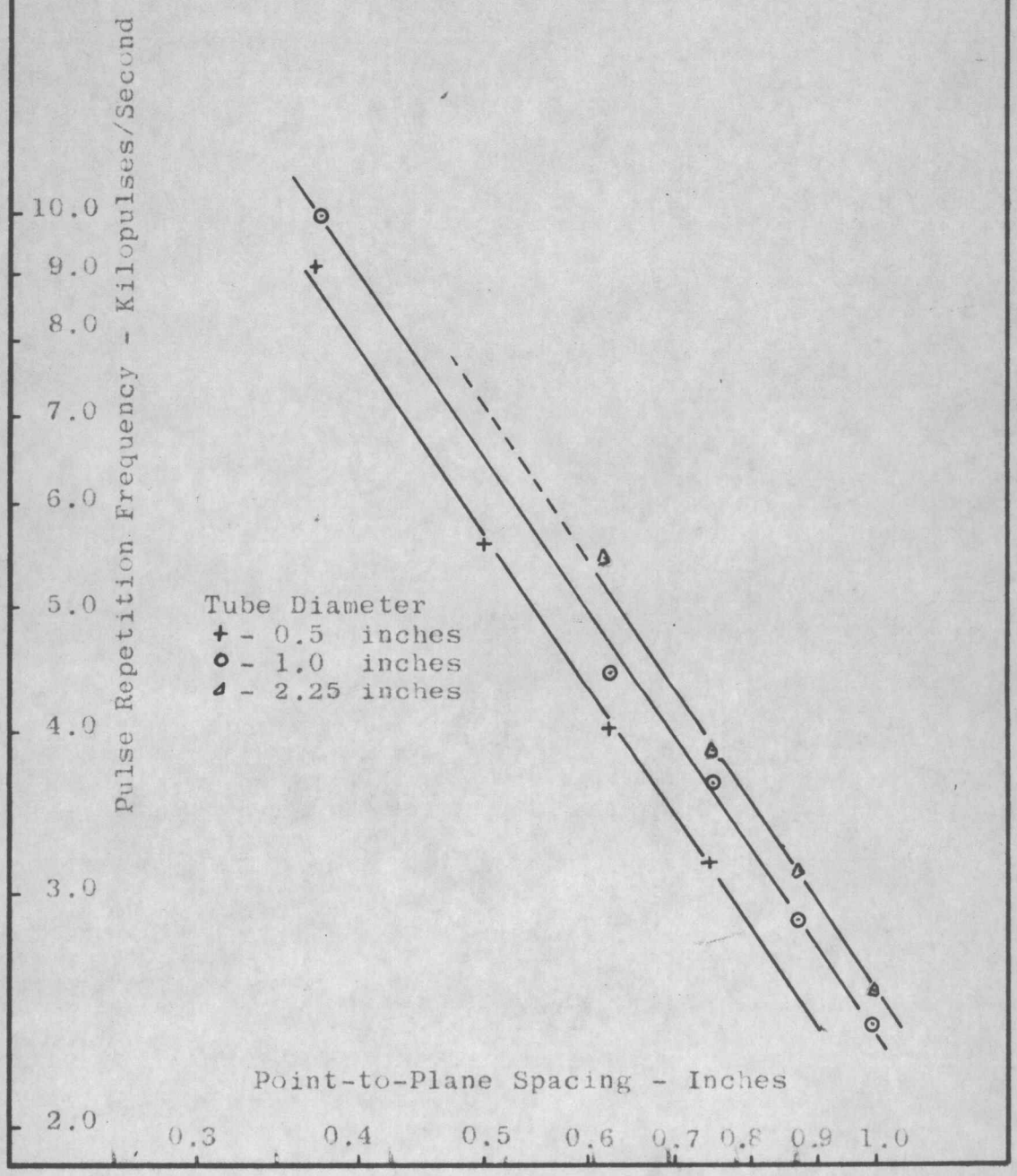

THEORY NEGATIVE POINT CORONA IMPULSES

Trichel's results made apparent the negative point corona (5) phenomena was dependent almost entirely upon the shape of the point and the conditions immediately surrounding the point.

When the negative point-to-plane potential reaches a critical value, there will exist a field near the point strong enough to give sufficient energy to a positive ion, in its last free path, to produce at least one secondary electron. A corona avalanche initiates when the free electrons proceed away from the point in a field strong enough to form new ions by inelastic collision with new molecules. The full effect of the liberated electrons is not felt until several ionizing free paths away from the point. At this time, the avalanche begins to recede for two reasons: First, the field weakens exponentially with distance from the point and second, because the electrons have left behind relative immobile positive ions whose space charge tends to reduce the field. Meanwhile, the positive ions are migrating toward the negative point, increasing the ionization in the region between the positive ion-space charge and the point. This decreases the ionization greatly between the positive ion-space charge and the plane electrode. When enough of the positive ion-space

charge has been dissipated near the negative point, the avalanche will start anew. This intermittent self-quenching discharge forms pulses which, as the negative point potential is raised a little further, become regularly spaced. The pulses resemble the output of a relaxation oscillator.

NEGATIVE POINT CORONA GENERATOR

The following discussion will pertain to a partial investigation of the characteristics of negative point corona. The basic goal was to establish a corona current pulse generator whose characteristics could be depended upon for investigative work. The investigation begins with the use of unshielded points of different radii. Tungsten (appendix I) was used to construct the hemispherical-shaped points, whose radii vary from 0.00945 to 0.00337 inches. The points are inserted into the hemispherical-shaped end of a one-fourth inch aluminum rod which forms the support for the point. The point tip extends one-half inch above the end of the rod. Measurements of the point, ion current, and repetition rates are made with a Tektronix-type 535 oscilloscope across resistors in the point-to-ground circuit. The point-to-plane gap spacing was 0.75 inches. It was found that this gap spacing allowed full range utilization of the high-voltage supply for the radii points being used.

Negative point corona was not audible; however, in total darkness a purplish color could be seen surrounding the point.

A sequence of photographs (figure 7) were made of the negative point corona. A variable-exposure photograph

sequence was necessary because of the intense light variation from the base of the corona umbrella to its outer edges. The left-hand photograph brings out the negative glow region and Faraday's dark space. Faraday's dark space is just above the negative glow. The glow region, to the eye, seems to be located directly on the point; however, there is a finite distance between the glow and the point. This is known as Crook's dark space. Figure 8 is a sketch of the corona (2,p.890) which gives a more realistic picture of the dark spaces. The second photograph shows the beginning of the corona umbrella, whereas the third photograph shows the entire umbrella. Had the microscope and camera contained quartz lenses instead of glass, the umbrella would have been larger.

During this microscopic investigation of the point, it was noticed that a grayish-white crystalline structure formed about the negative-glow spot on the point. The crystals would form a ring around the point and then build up inwardly so as to decrease the area inside the ring. Once the ring had formed, the negative glow region would move outside the ring to a new position on the point radius. The rate at which the crystals form depends upon the gradient at the point. With about fifty microamperes of ion current, the crystals formed in a few minutes. When the crystals were removed, by washing the point in acetone,

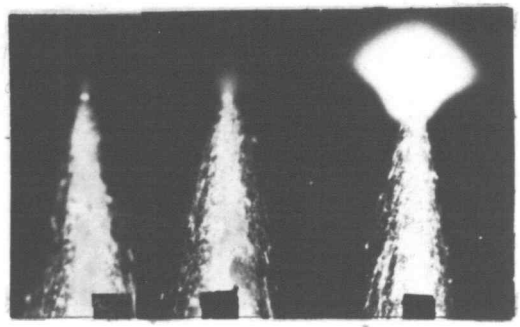

Figure 7. The negative point corona was photographed in three steps to show the different parts of the corona umbrella. (Left-right, 1-7 second exposure with Kodak, Royal-X-Pan film)

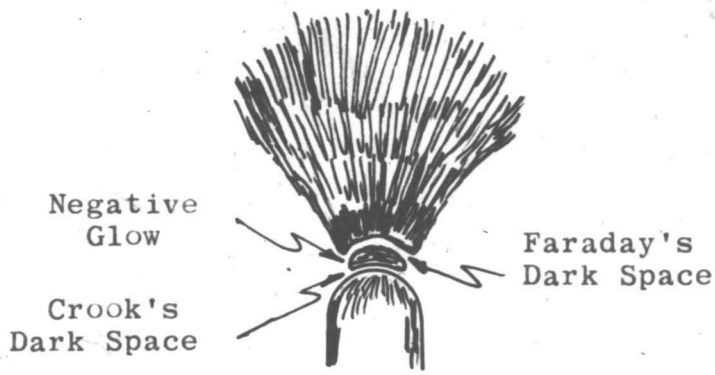

Figure 8. Sketch of negative point corona umbrella.

the negative glow would return to its original position on the point. As will be shown later, these crystals distort the characteristics of the corona generator.

Negative point corona was quite stable over a wide variation of point-to-plane voltage for a fixed point-to-plane configuration. Where the positive point corona would flashover with a one to four kilovolt change above corona onset, the negative point-to-plane voltage could change as much as fourteen kilovolts above onset without flashover. This essentially gives, for a specific gap arrangement, an easy method of changing the field surrounding a point without making adjustments in the point-to-plane spacing. Basically, controlling the field surrounding the point meant controlling the repetition rate of the current pulses. The pulses became more uniform with a high clearing field surrounding the point. The upper limit to the intensity of the clearing field is determined by the point-to-plane flashover voltage.

Figure 9-a,b,c, and d shows the effect of the increasing gradient of the point. The second pulse of the first photograph (figure 9-a) is indistinct because at this voltage the relaxation period is irregular. As the clearing field at the point was increased, the repetition period became well regulated at 18,000 volts. With a high clearing field, the repetitive pulses will appear as

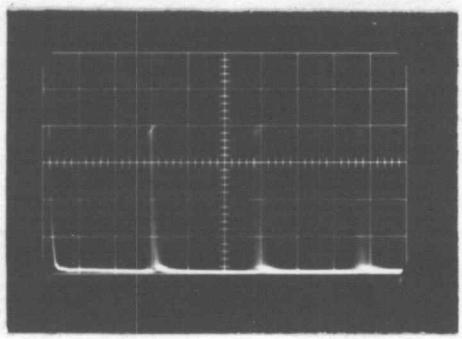

Figure 9-a. Es = 12 kv

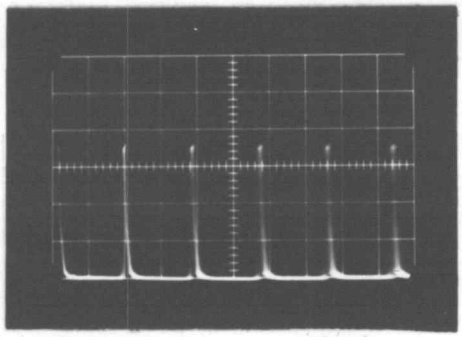

Figure 9-b. Es = 14 kv

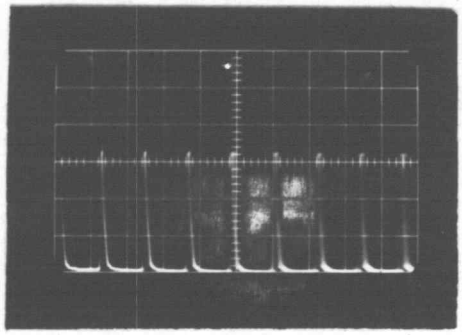

Figure 9-c. Es = 16 kv

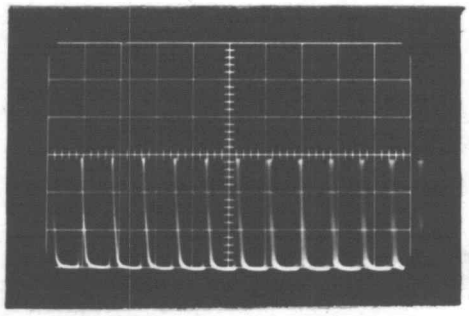

Figure 9-d. Es = 18 kv

Figures 9-a,b,c and d show the effect of increasing negative point-to-plane voltage on the pulse repetition period and pulse shape.
gap spacing - 0.75 inches
time scale - 1 micro-sec/cm
voltage scale - 0.05 v/cm

figure 9-d. The rise and decay times of the pulse displayed in figure 10 are not indicative of the true rise and decay time of the actual electron avalanche. The wave shape was influenced by the measuring circuit. Rise time, on the order of 2×10^{-8} seconds, could be observed with the Tektronix-type 535 oscilloscope by using the fast rise (0.006 microseconds) type (53/54k) vertical amplifier plug-in unit.

For a particular point-to-plane voltage, point radius, and gap spacing, there were three measurable parameters that helped describe the corona generator's characteristics. Pulse repetition period, pulse height, and ion current were measured with an oscilloscope across resistors in the point circuit.

Figure 11 shows the pulse repetition frequency as a linear function of the ion current in the point circuit. For high values of ion current, the negative spot will begin to move around the point because of the previous mentioned crystal ring. This will cause the repetition period to continually shift. The curves of figure 11 shift up or down depending on the effective radius at the immediate location of the negative glow spot. Washing the point in acetone and quickly recording the repetition periods at high values of current will minimize the error introduced

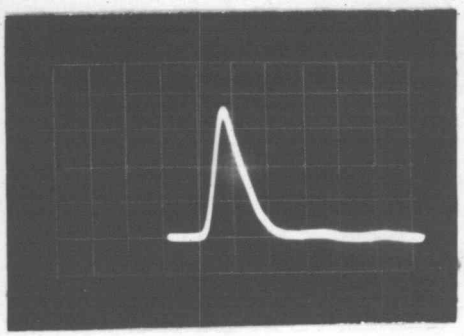

Figure 10. A negative point-to-plane current pulse.(Time-0.1μ sec./cm, voltage-0.05 v/cm, 16 kv-point voltage, 0.75 inch-gap.)

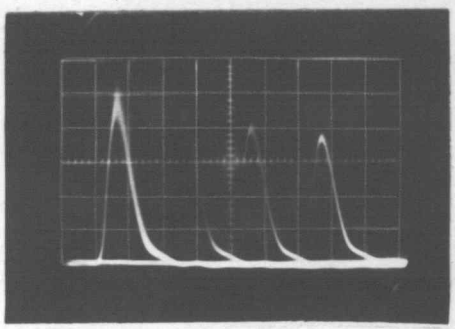

Figure 13. A multiple exposure photograph showing the decreasing pulse height with increasing negative point-to-plane voltage. (Left-right, Es = 6,8,10,12-kv. Time - 0.01μ sec/cm, voltage - 0.05 v/cm.)

Figure 11

PULSE REPETITION FREQUENCY AS
A FUNCTION OF POINT-ION CURRENT

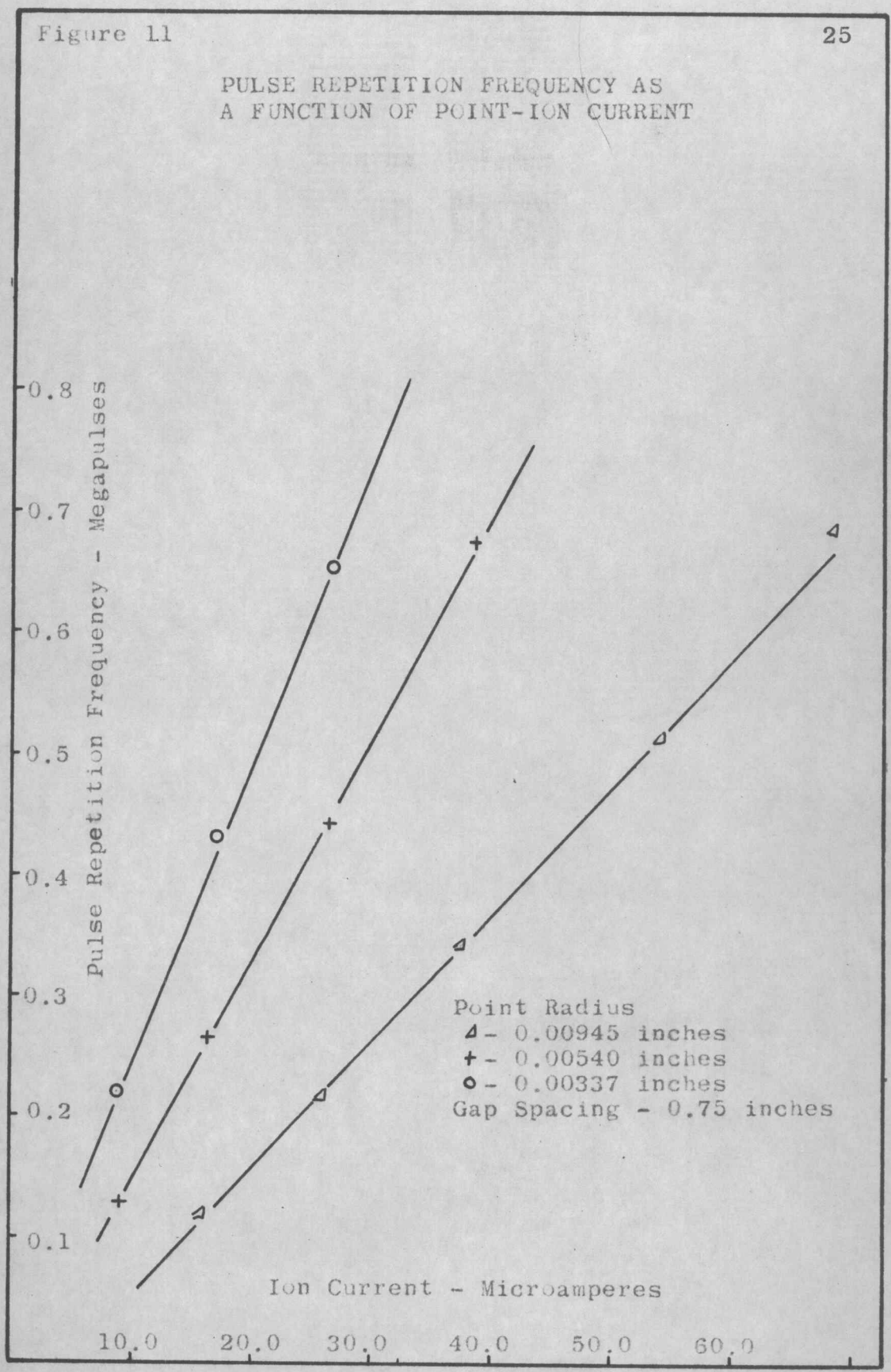

by the crystals. This essentially means that the repetition frequency will not remain constant over a period of time for a particular point-to-plane voltage and gap configuration. It is not possible to extend the curves to zero because the normal glow corona ceases to exist below a certain voltage level.

The upper limit of the curve is determined by the flashover voltage. The possible frequency limit with the radii point used in this test was between 50 kilopulses per second and one megapulse per second. This repetition frequency range is between the frequencies for which the NEMA circuit has been tuned.

Figure 12 shows the pulse repetition frequency plotted as a function of point-to-plane potential for a fixed point radius and gap spacing. The equation for this curve is a cubic function.

equation 1.

$$\text{Repetition frequency} = a\left[(\text{point voltage})\right]^3 \text{ megapulses per second}$$

where the constant (a) is dependent upon the point radius.

This curve was the most convenient to use when a particular pulse repetition frequency was desired, because of the ease with which the supply voltage could be adjusted.

Figure 12

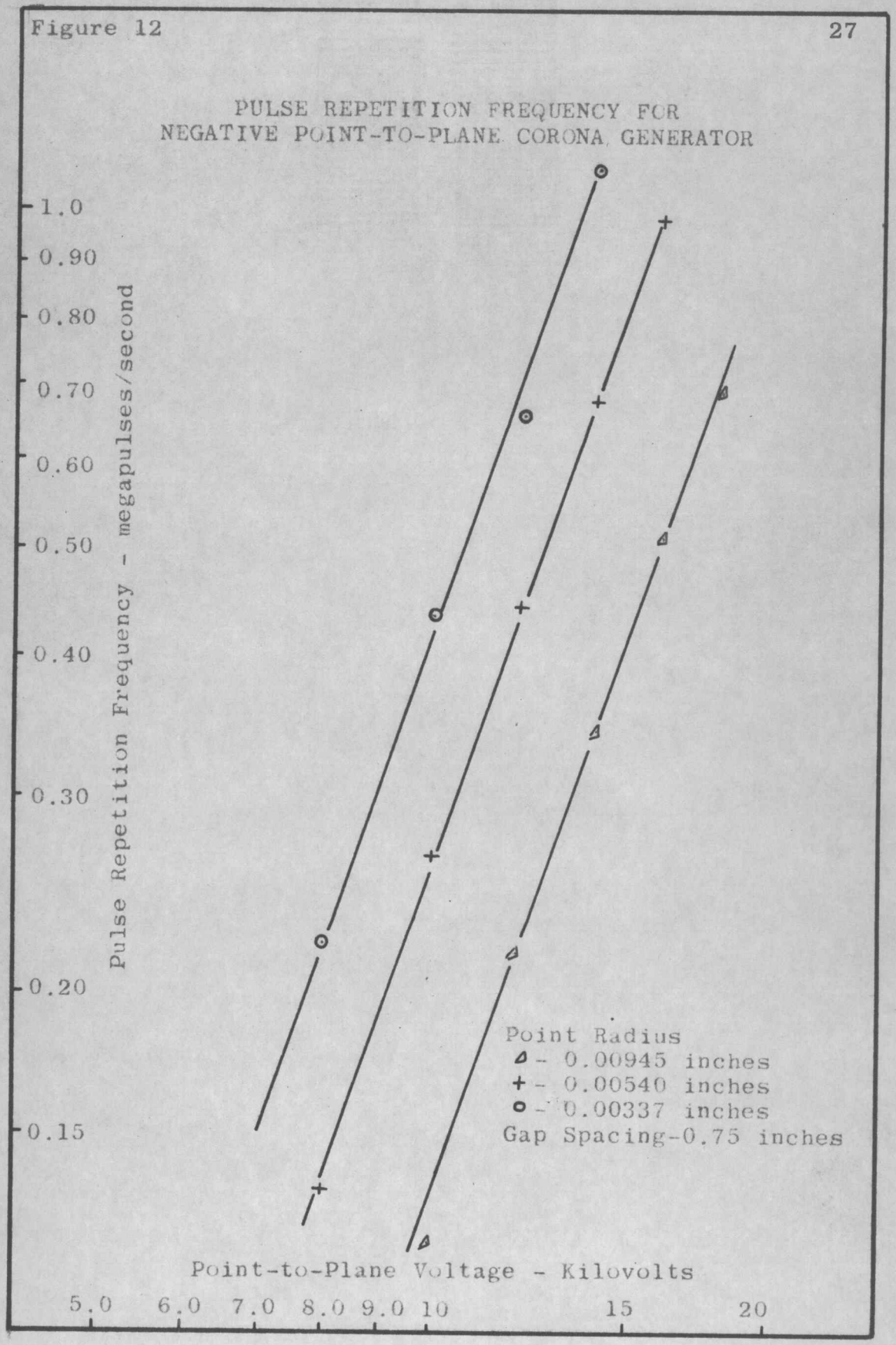
PULSE REPETITION FREQUENCY FOR
NEGATIVE POINT-TO-PLANE CORONA GENERATOR
Pulse Repetition Frequency - megapulses/second
1.0
0.90
0.80
0.70
0.60
0.50
0.40
0.30
0.20
0.15
Point Radius
- 0.00945 inches
+ - 0.00540 inches
o - 0.00337 inches
Gap Spacing-0.75 inches
Point-to-Plane Voltage - Kilovolts
5.0
6.0
7.0
8.0
9.0
10
15
20

The multiple-exposure photograph in figure 13 was taken to show the pulse height change versus the point-to-plane voltage. The pulse on the left, in figure 13, was photographed at a particular point-to-plane voltage and then the point voltage was increased and the oscilloscope trace was moved horizontally to the position of the second pulse. Figure 14 is a plot of pulse height as a function of increasing point voltage for a constant radius and gap spacing. The equation for the curve is a decaying exponential function.

Figure 14.

NEGATIVE POINT-TO-PLANE
PULSE HEIGHT

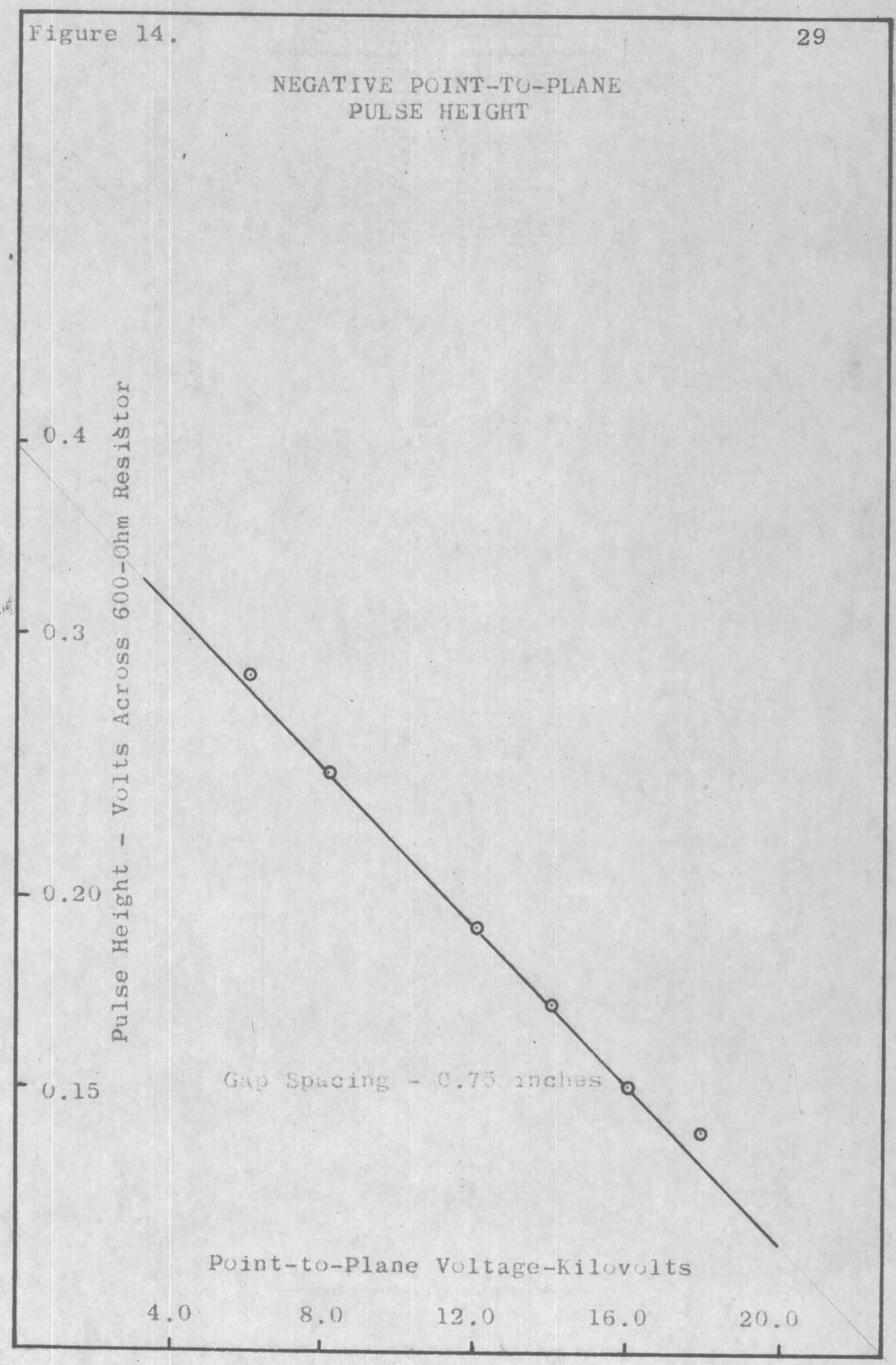

RADIO NOISE CHARACTERISTICS OF POSITIVE D-C POINT-TO-PLANE CORONA

The positive point-to-plane corona generator is easily flashed over. The allowable variation in the supply voltage, with an 0.75-inch gap, is one to four kilovolts beyond onset before flashover occurs. This restricted the measurement of radio noise characteristics of the corona pulses to a narrow point-to-plane voltage range. The radio noise measured in this narrow voltage range describes the possible magnitude of radio noise near onset. It was difficult to make a comparison of radio noise for the same point because of the deviation in onset voltages. At one time, the positive corona may start at 10,000 volts, and the next time at 11,000 volts. This variation in onset voltages is due to the nature of the starting mechanism of positive corona. The positive corona starting mechanism is photoelectric ionization caused by an electron avalanche toward the point. This self-sustaining ionization does not occur at the same voltage each time (1,p.522). Measured values of positive-point corona radio noise, just beyond onset, will increase considerably. In the small region in which observations of the radio noise could be made, there seemed to be no upper limit before flashover. The microvolts of radio

noise for a 0.75-inch gap and an 0.0065-inch point radius increased from 2 x 10^3 QP microvolts to 20 x 10^3 QP microvolts for a 1.3 kv increase in supply voltage. As a comparison, it requires an increase of 8 kv beyond onset to get the same change in radio noise from a negative point.

RADIO NOISE CHARACTERISTICS OF NEGATIVE DIRECT CURRENT POINT-TO-PLANE CORONA

Radio noise characteristics of negative point-to-plane corona were measured at the four frequencies (0.71, 0.83, 2.28, 3.18 MC) for which the NEMA circuit was tuned and at 0.83 MC with five different resistors (75, 150, 300, 600, 1000 ohms) in the point circuit.

A Stoddart radio interference-field intensity meter was used to measure microvolts of radio noise generated by the corona pulses. The Stoddart meter, which is a frequency selective microvolt meter, was coupled across a resistor in the point circuit. The indicated microvolts of radio noise produced by the current pulses were recorded, using the quasi-peak function on the Stoddart meter. In the quasi-peak function, the time constants of the detector circuits approach one-millisecond charge time and 600-millisecond discharge time (4, p.8). This gives a meter indication near the peak value of the interfering signal. The five resistive terminations for the Oregon State College NEMA circuit were used in the corona generator's point circuit. As will be demonstrated later, the magnitude of radio noise generated by the corona current pulses was dependent upon the size of the point circuit resistor.

It is difficult to measure the radio noise characteristics of a particular gap configuration by taking step-by-step changes in the point-to-plane potential. The reason for this is that the pulse repetition frequency for the points will begin to shift after being used a few minutes. To insure the accuracy of Stoddart meter indications for a particular point voltage setting, it was necessary to clean the point in acetone and take the indicated radio noise reading immediately. This method required a considerable amount of time and the results were not too accurate because by taking step-by-step changes in the supply voltage, there was a chance of passing over any irregular change in the radio noise reading.

An expeditious procedure for recording the pulse radio noise characteristics was developed by using the time constant of the power supply and the external meter connection on the Stoddart meter. Because of the power supply time constant, the output potential will decrease exponentially from 18,000 volts to near zero in about 25 seconds. The empirical equation for the output voltage of the power supply is:

equation 2

$$E_{(out)} = 18{,}000\epsilon^{-(0.1835\ t)} \text{ volts,}$$

where (t) is in seconds.

By means of the external meter receptacle (J 106) on the Stoddart meter, another type of recording device was added in series with the (0-1 ma) ammeter (M-101). The addition of the external instrument had no effect on the (0-1 ma) ammeter as long as the resistance of the added instrument was 1500 ohms. A 1500-ohm resistor was added to the external meter circuit and voltage readings were made across the resistor with an oscilloscope. The voltage readings were then calibrated against the readings of the Stoddart meter. The oscilloscope was externally triggered by the power supply switch so that the elapsed decay time of the power supply could be read from the oscilloscope trace. Once the oscilloscope had been triggered by the power-supply switch, the time axis of the oscilloscope represented the exponentially decreasing point-to-plane voltage. By using the elapsed decay time, the power-supply voltage can be computed from equation 2. By adjusting the oscilloscope sweep time to correspond with the decay time of the power supply, an oscilloscope trace of all radio noise indications from 18,000 volts to near zero was observed in ten to twenty seconds. This information was recorded with a photograph of the oscilloscope trace. With this method of recording radio noise, the point-to-plane voltage had to be applied for only a short period of time. This avoids the errors introduced by the shifting pulse repetition frequency.

It is possible to combine equations one and two into an empirical equation which will describe the repetition frequency at any time after the oscilloscope has been triggered. The expression resulting from the combination of the two equations is:

Equation 3

$$F = a\left[18{,}000\,\epsilon^{-(0.1835t)}\right]^3 \text{ pulses/second}$$

Where (F) is the pulse repetition frequency
(t) is the elapsed time after the oscilloscope was triggered
(a) is a constant dependent upon the point radius.

If a point radius would not change and could be used over and over again, the constant (a) of equation 3 could be evaluated. The point radius does change, however, and the intercept (a) will change accordingly (see figure 12). To avoid computing new values of (a) for each point radius, it was simpler to shift the zero-time axis of the oscilloscope trace and leave the constant (a) fixed. The constant (a) has been evaluated for a particular point radius in equation 4.

Equation 4

$$F = 0.217 \times 10^{-6}\left[18{,}000\,\epsilon^{-(0.1835\ t)}\right]^3 \text{ mega-pulses/second}$$

To use equation four for positioning the zero-time axis, for a particular pulse repetition frequency, the pulse repetition frequency must be known to exist at a point-to-plane

voltage less than 18,000 volts. This can be quickly checked on the oscilloscope.

An example of placing the zero-time axis for 0.83 megapulses (figure 15-a) is as follows: (Stoddart meter is also tuned for 0.83 MC). Replace (F) in equation four with 0.83 megapulses and solve for (t). In this case, (t) is equal to 0.76 seconds. This means that the zero-time axis is located on figure 15-a, 0.76 seconds to the left of the radio noise deflection at 0.83 megapulses. For frequencies set on the Stoddart meter that are above the pulse repetition frequency band, the zero-time axis will have to be computed for some frequency that does fall within the pulse band and whose harmonic is equal to the meter frequency. For example, the pulse band does not include 2.28 MC, but it does include 1.14 MC, of which the 2.28 MC frequency is the second harmonic. Computing (t) from equation four, using (F) equal to 1.14 megapulses, will give 0.187 seconds. The zero-time axis is located in figure 15-g, 0.187 seconds to the left of the radio noise deflection at 1.14 megapulses. By measuring the time elapsed from the zero-time axis to any radio noise deflection, the pulse repetition frequency that caused the deflection can be computed from equation four.

RIV-Corona Gen. (Output)

RIV-NEMA Ckt. (Output)

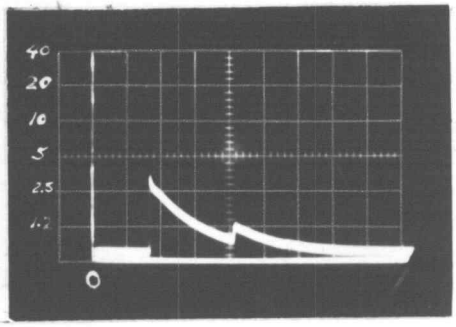

(a)
0.83MC
75-ohm
resistor

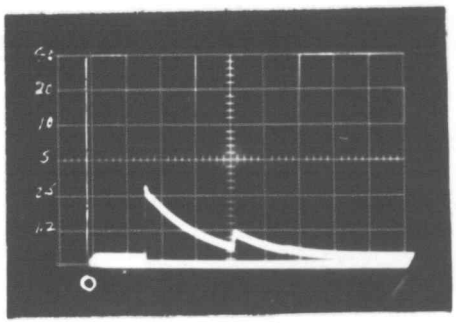

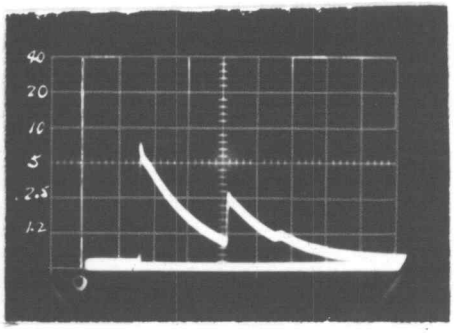

(b)
0.83MC
150-ohm
resistor

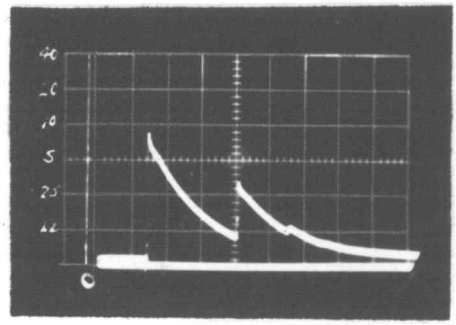

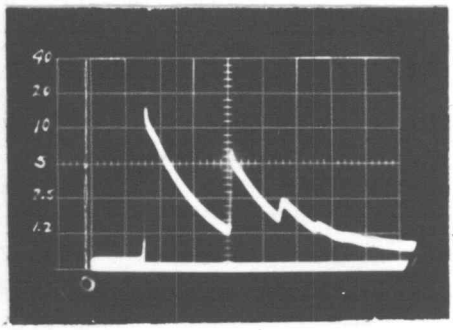

(c)
0.83MC
300-ohm
resistor

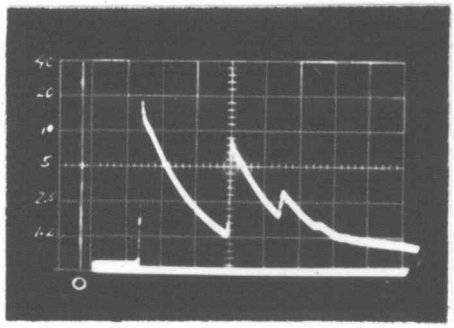

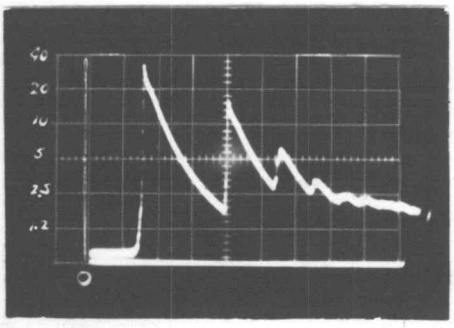

(d)
0.83MC
600-ohm
resistor

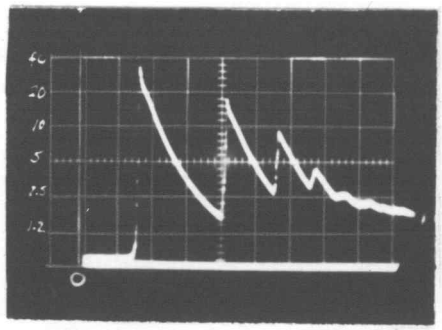

Figure 15. R-I voltage output from negative point corona generator. (Time - 500 ms/cm volts - QP x 10^3 volts.)

Figure 16. R-I voltage output from NEMA circuit with negative point corona gen. on input. (Time - 500 ms/cm volts - QP x 10^3 volts.)

RIV-Corona Gen. (Output)

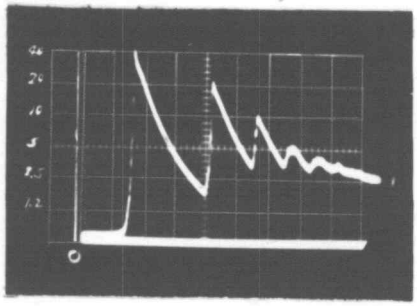

(e)
0.83MC
1000-ohm
resistor

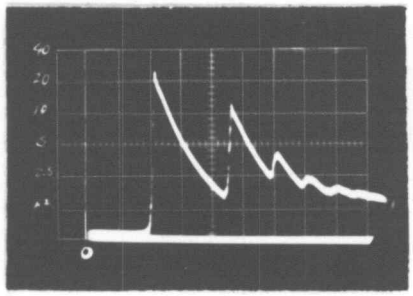

(f)
0.71MC
600-ohm
resistor

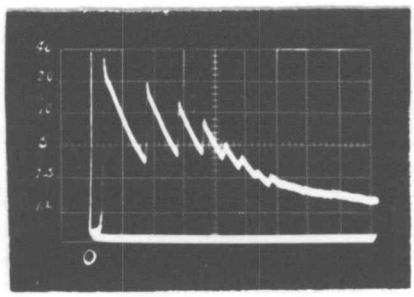

(g)
2.28MC
600-ohm
resistor

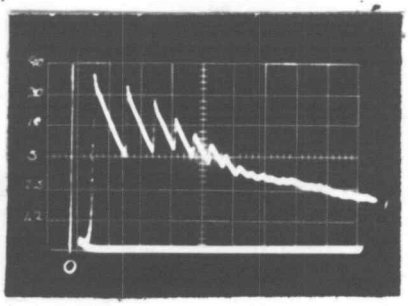

(h)
3.18MC
600-ohm
resistor

Figure 15. R-I voltage output from negative point corona generator. (Time - 500 ms/cm volts - QP x 10^3 volts.)

RIV-NEMA Ckt. (Output)

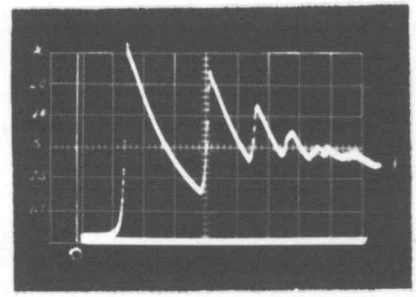

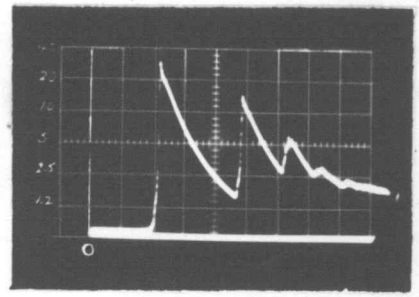

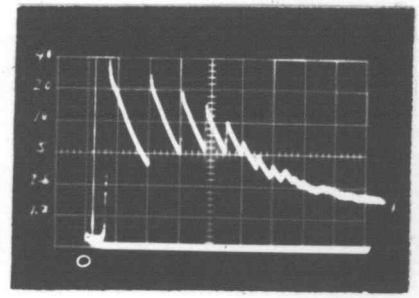

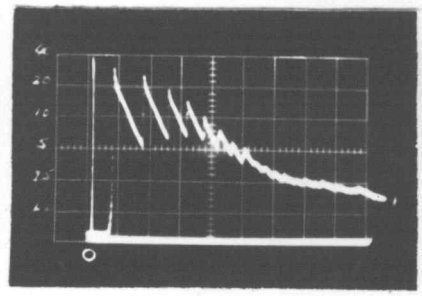

Figure 16. R-I voltage output from NEMA circuit with negative point corona gen. on input. (Time - 500 ms/cm volts - QP x 10^3 volts.)

Compiled in Table I are the pulse repetition frequencies and the microvolts (RIV) of radio noise from the oscillograms of figure 15.

Under the "pulse frequency" column are listed the pulse repetition frequencies that occurred as the power supply voltage was decreasing exponentially from 18,000 volts. The radio noise indication for the frequency set on the Stoddart meter was due to the same pulse repetition frequency or harmonics of lesser pulse repetition frequencies.

For the 0.83 MC Stoddart meter frequency, the first pulse was due to a pulse repetition frequency of 0.83 megapulses/second. This can easily be checked with the oscilloscope. The second radio noise deflection was the result of the second harmonic of 0.415 megapulses/second. For the 2.28 MC frequency, the first pulse was caused by the second harmonic of 1.14 megapulses/second. The 2.28 MC pulse repetition frequency was outside the pulse band for the particular gap configuration, so it could not have caused the first radio noise deflection. This is also true for the 3.18 MC setting on the Stoddart meter. The first radio noise indication is caused by the 1.06 megapulse/second frequency of which 3.18 MC is the third harmonic.

TABLE I

NEGATIVE POINT CORONA RADIO NOISE CHARACTERISTICS AND THE CONDUCTED RADIO NOISE OF THE NEMA CIRCUIT

Stoddart Meter Frequency Mcps	N-P Gen. Point Ckt. Resistor	Corona Pulse Rep-Freq. Megapulses/ Second	N-P Gen. RIV-μvQP	NEMA Circuit Conducted RIV-μvQP
0.83	75 ohms	0.83	3.5×10^3	3.0×10^3
		0.415	1.3	1.2
		0.276		
		0.207		
0.83	150 ohms	0.83	7.7×10^3	8.5×10^3
		0.415	2.8	3.2
		0.276	1.3	1.4
		0.207		
0.83	300 ohms	0.83	15.0×10^3	16.0×10^3
		0.415	6.7	8.7
		0.276	2.5	3.2
		0.207	1.6	1.6
0.83	600 ohms	0.83	35.0×10^3	35.0×10^3
		0.415	16.0	17.0
		0.276	6.6	10.0
		0.207	3.2	4.2
0.83	1000 ohms	0.83	47.0×10^3	50.0×10^3
		0.415	23.0	26.0
		0.276	10.5	13.0
		0.207	5.3	7.0
0.71	600 ohms	0.71	25.0×10^3	25.0×10^3
		0.355	12.0	15.0
		0.233	4.4	5.4
		0.170	2.4	3.0
2.28	600 ohms	1.14	33.0×10^3	40.0×10^3
		0.760	20.0	27.0
		0.570	14.0	20.0
		0.456	8.7	13.0
		0.380	5.0	6.0
3.18	600 ohms	1.06	30.0	30.0
		0.795	24.0	25.0
		0.636	18.0	20.0
		0.530	12.0	15.0
		0.454	8.0	7.8

The abrupt Stoddart meter deflections become indistinct when the point-to-plane voltage decreases to about 10,000 volts. The reason for this is the irregularity of the pulse repetition frequency. At low point-to-plane voltages, the pulse repetition frequency becomes sporadic because the field about the point is not strong enough to insure secondary electron emission by positive ion bombardment (1, p.517). The radio noise generated by the corona generator below 10,000 volts was due to the random electron avalanches.

As Table I indicates for the 0.83 MC frequency, the radio noise generated by a constant corona pulse frequency across different value resistors is directly proportional to the value of the resistor. This shows that the corona generator is essentially a current source.

OREGON STATE COLLEGE NEMA CIRCUIT

The circuit which has been pulsed with the current-pulse generator is termed the "NEMA" circuit. The National Electrical Manufactors Association (NEMA) has established a standard (3) circuit for measuring radio-influence voltages from 60-cycle high voltage sources. Figure 17 is a modified version of the recommended NEMA circuit, which is located in the high-voltage laboratory at Oregon State College. The modification of the NEMA circuit was necessary because of the stray capacitance between the coupling capacitor base and ground. The modification was the addition of a tuned circuit to isolate the coupling capacitor base above ground for radio frequencies.

The circuit is tuned for four frequencies (0.71, 0.83, 2.28, 3.18 MC) with a single frequency (0.83 MC) available with five resistive terminations (75, 150, 300, 600, 1000 ohms).

Figures 18 and 19 show the location of the NEMA circuit components in the laboratory. The choke coil (L1) is located in a stainless-steel bus that connects the high-voltage transformer to the insulator pedestal. The NEMA coupling capacitor (C_1 - 0.001266 μf) is located to the right in figure 18. Inductor (L2) and (L3) are housed in seperate metal boxes attached to the base of the coupling capacitor. Inductor (L4) and resistor terminations

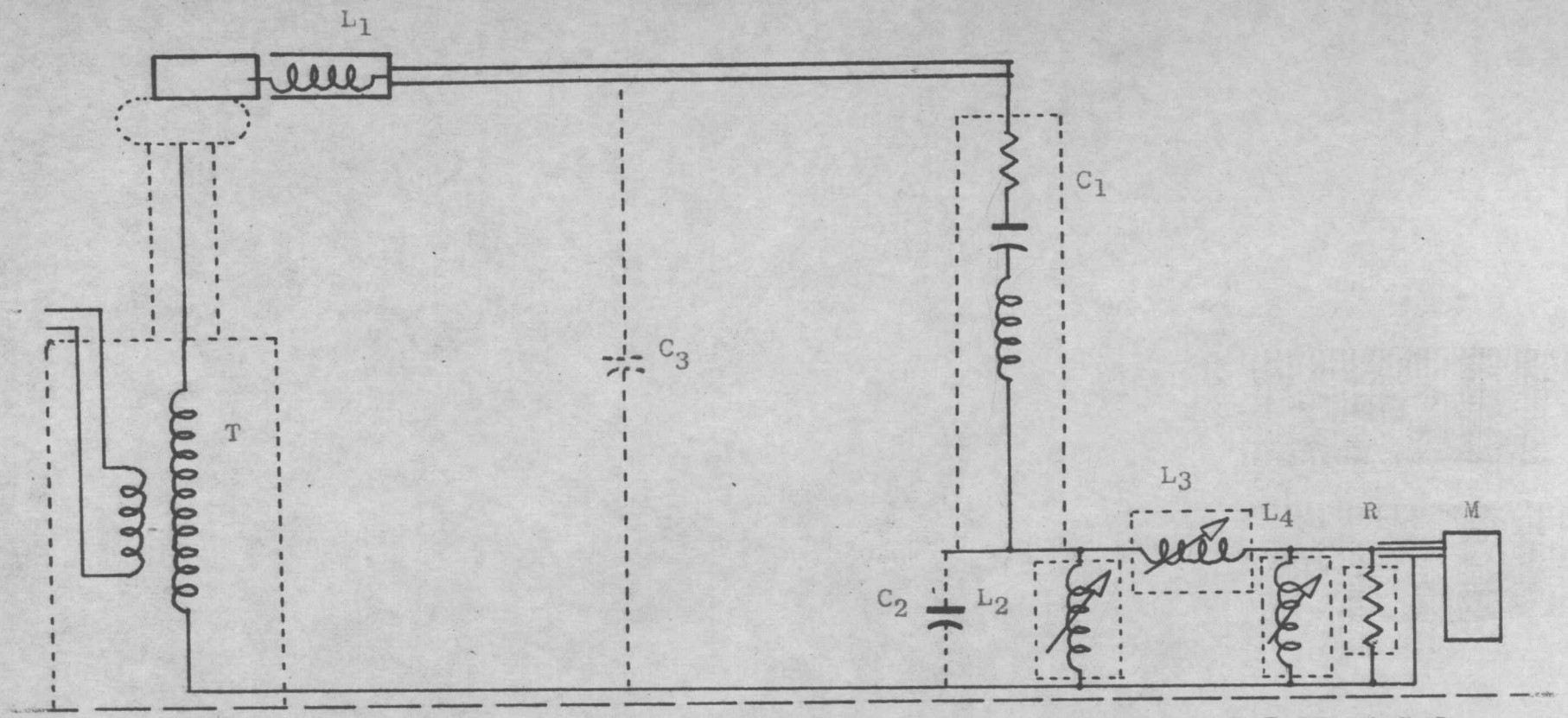

Figure 17. SCHEMATIC DIAGRAM OF THE NEMA CIRCUIT, HIGH-VOLTAGE LABORATORY, O.S.C.

T - 350,000 volt transformer
L_1 - Isolating choke coil
C_1 - Capacitor stack
L_2 - Base coil
C_2 - Base capacitance
L_3 - Series coil
C_3 - Distributed capacitance
L_4 - Shunt coil
R - Shunt resistance
M - Stoddart RI-FI meter

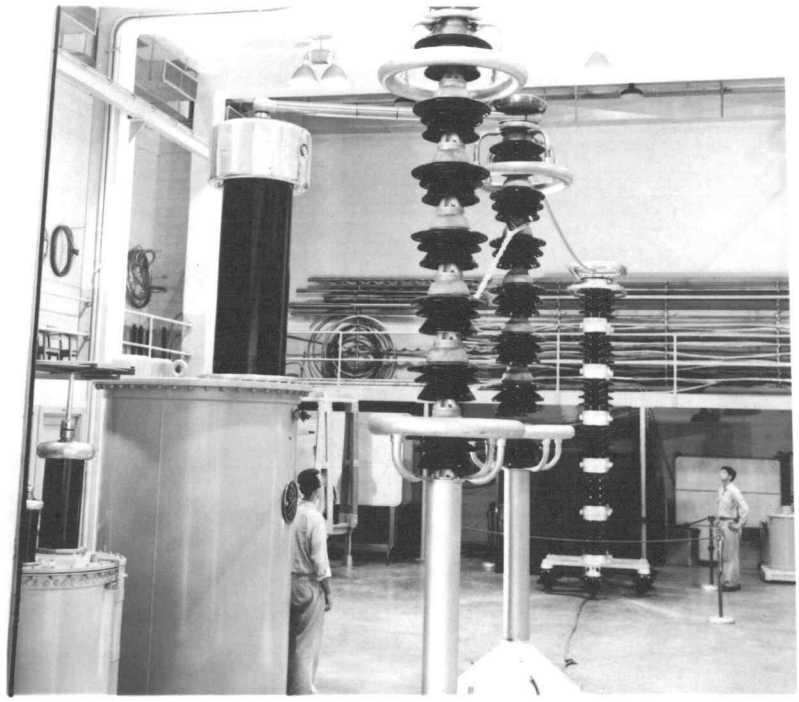

Figure 18. High-voltage laboratory showing NEMA capacitor stack, in right background.

Figure 19. High-voltage laboratory showing 350 kv transformer and insulator pedestal, in left background.

are located inside the shielded cage at the far end of the upper photograph.

The NEMA circuit was tuned for the four frequencies in this manner: The choke coils were individually constructed and placed in a section of stainless-steel bus with a selection switch. Impedance measurements were then made on the coils, independent of the NEMA circuit. Figures 20-23 show that the inductive reactances for three coils at frequencies 0.71, 0.83, and 2.28 MC are twenty-thousand ohms or above. The inductive reactance of the 3.18 MC coil did not quite make twenty-thousand ohms.

The stray capacitance of the coupling capacitor base to ground was parallel tuned by inductor L_2. While the base was being tuned, the conductor from the coupling capacitor to the insulator pedestal was disconnected as well as the inductor L_4 and terminating resistor (R).

Coupling capacitor C_1 was series tuned by inductor L_3 while the conductor and resistor termination were disconnected. The final step was the parallel tuning of C_3 by inductor L_4. For this step, the choked section of the transformer bus and resistor termination were removed. Characteristics of the overall circuit to frequencies, for which it was tuned, (600 ohm termination) appear in figures 24-27.

Figure 20

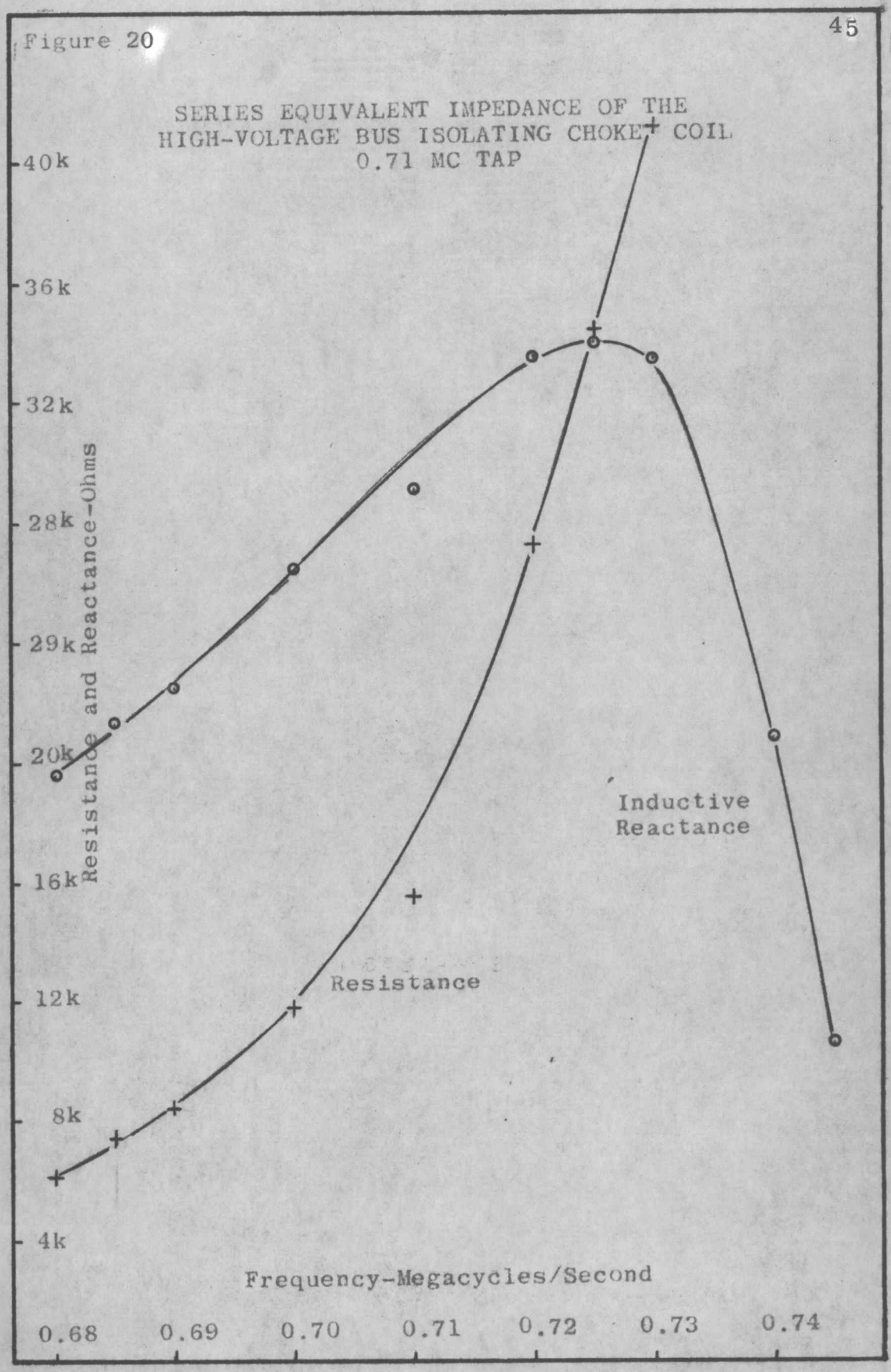
SERIES EQUIVALENT IMPEDANCE OF THE
HIGH-VOLTAGE BUS ISOLATING CHOKE COIL
0.71 MC TAP
40k
36k
32k
28k
29k
20k
16k
12k
8k
4k
Resistance and Reactance-Ohms
Inductive
Reactance
Resistance
Frequency-Megacycles/Second
0.68
0.69
0.70
0.71
0.72
0.73
0.74

Figure 21

SERIES EQUIVALENT IMPEDANCE OF THE
HIGH-VOLTAGE BUS ISOLATING CHOKE COIL
0.83 MC TAP

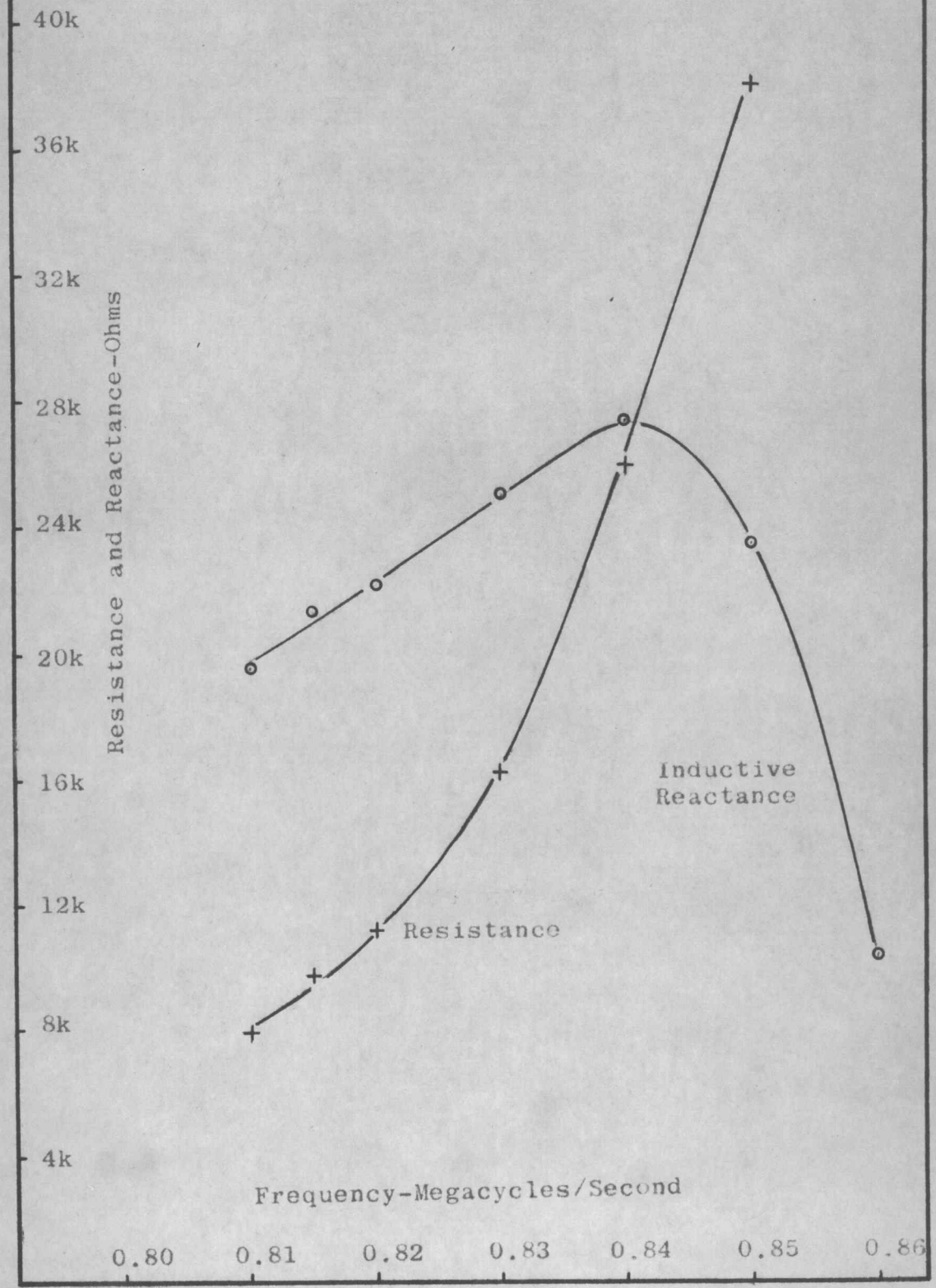

Figure 22

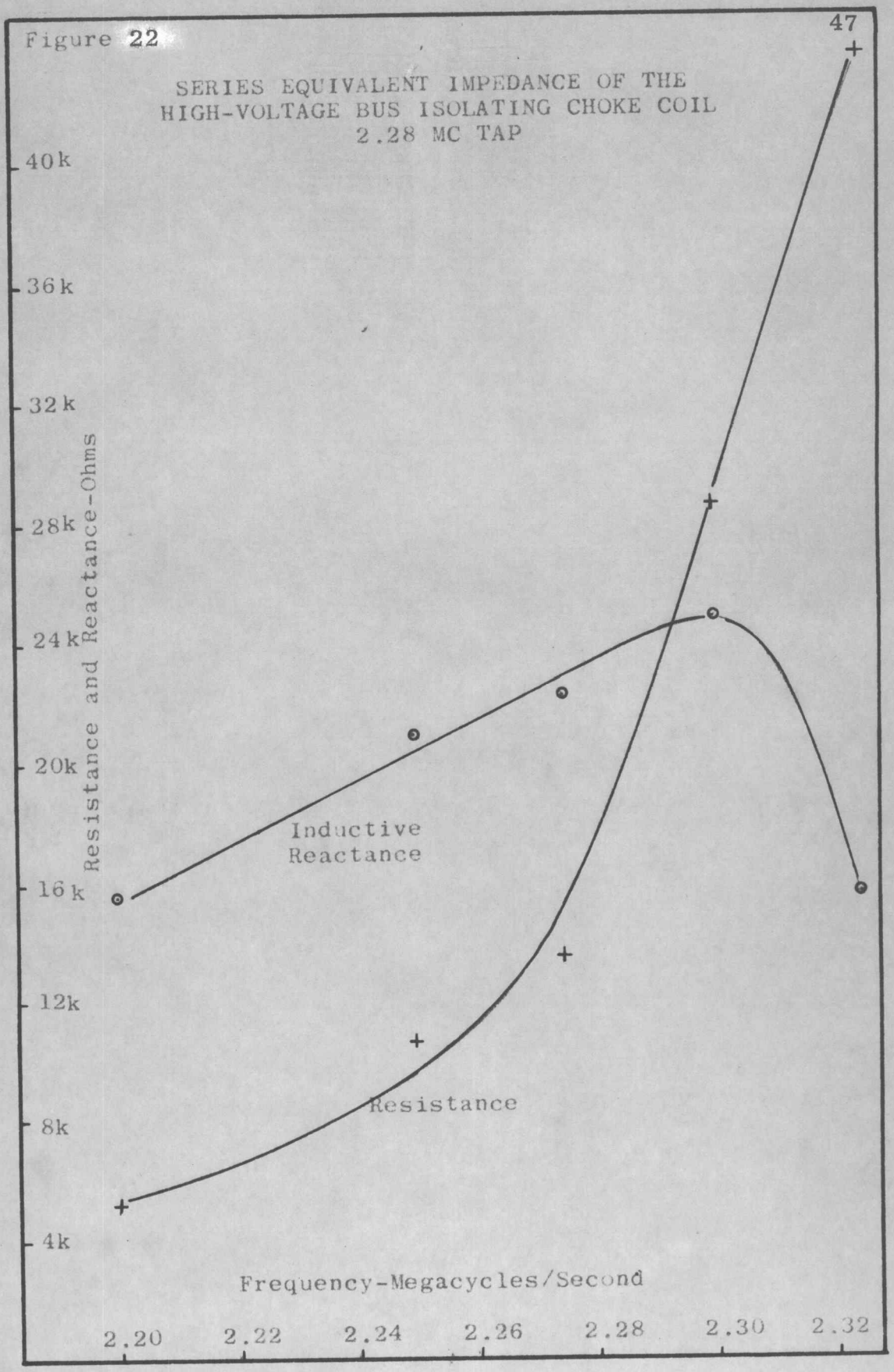
SERIES EQUIVALENT IMPEDANCE OF THE
HIGH-VOLTAGE BUS ISOLATING CHOKE COIL
2.28 MC TAP
40k
36k
32k
28k
24k
20k
16k
12k
8k
4k
Resistance and Reactance-Ohms
Inductive
Reactance
Resistance
Frequency-Megacycles/Second
2.20
2.22
2.24
2.26
2.28
2.30
2.32

Figure 23

SERIES EQUIVALENT IMPEDANCE OF THE
HIGH-VOLTAGE BUS ISOLATING CHOKE COIL
3.18 MC TAP

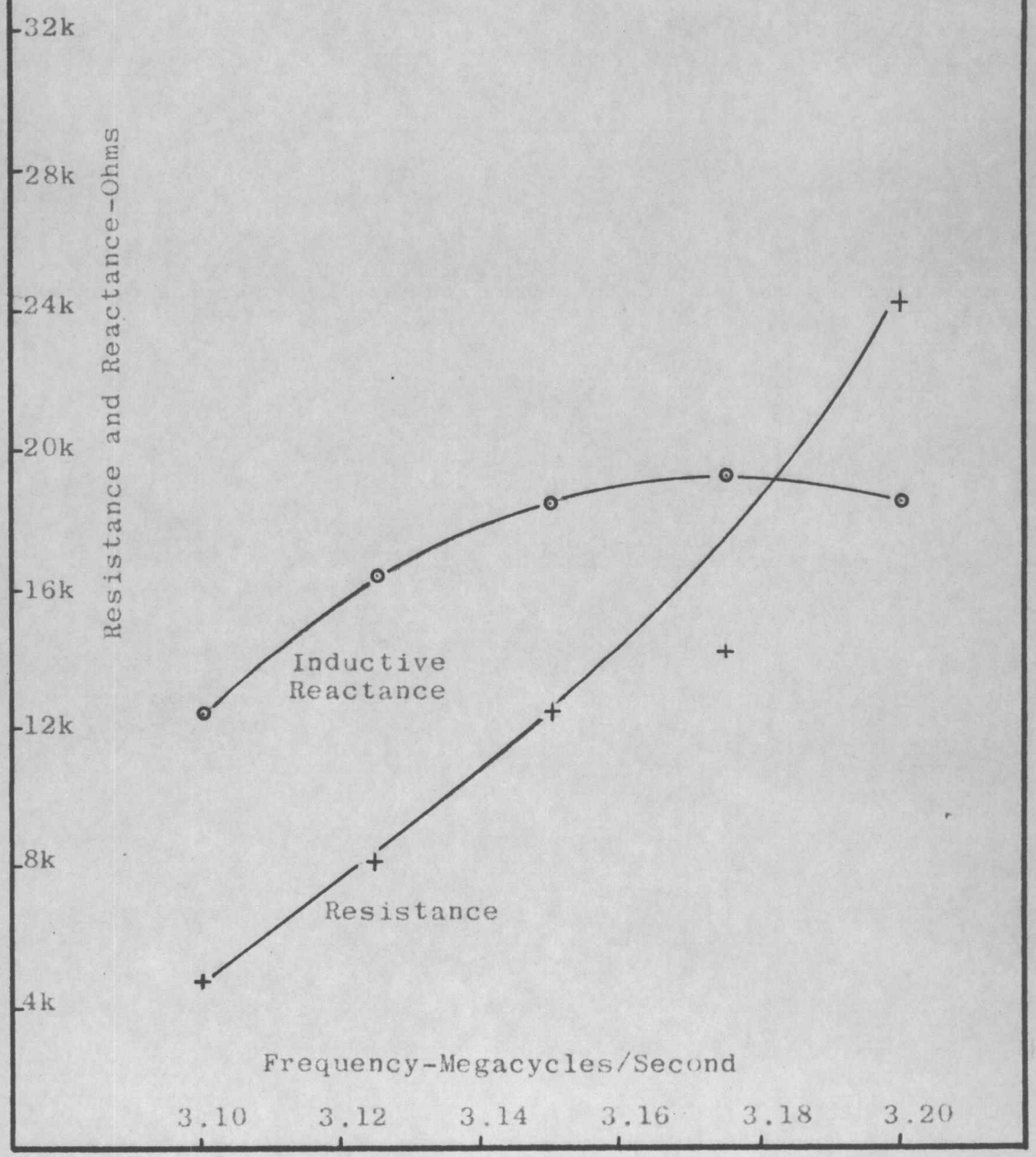

Figure 24

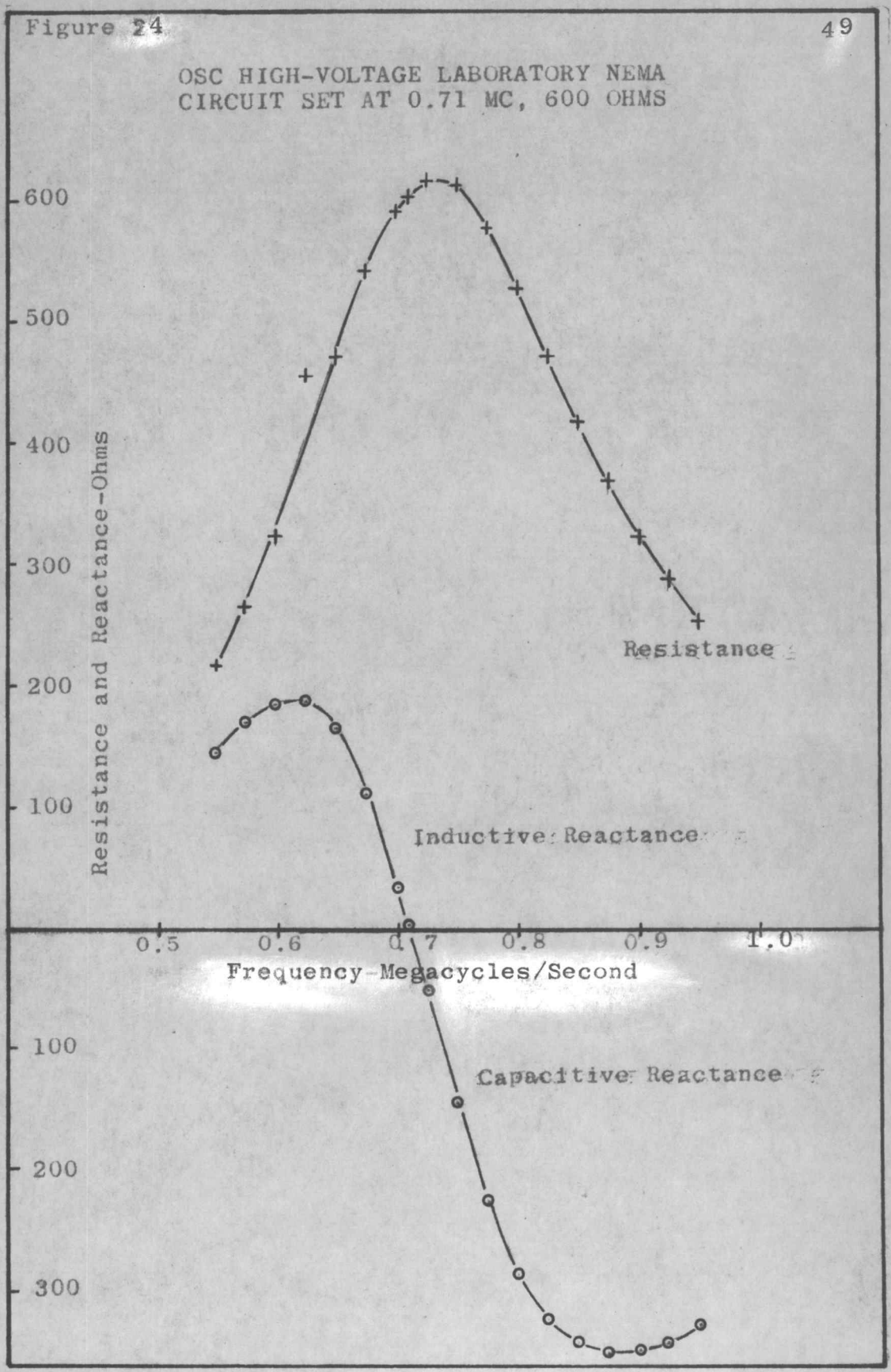
OSC HIGH-VOLTAGE LABORATORY NEMA
CIRCUIT SET AT 0.71 MC, 600 OHMS
600
500
400
300
200
100
Resistance and Reactance-Ohms
Resistance
Inductive Reactance
0.5
0.6
0.7
0.8
0.9
1.0
Frequency-Megacycles/Second
100
200
300
Capacitive Reactance

Figure 25

OSC HIGH-VOLTAGE LABORATORY NEMA
CIRCUIT SET AT 0.830 MC, 600 OHMS

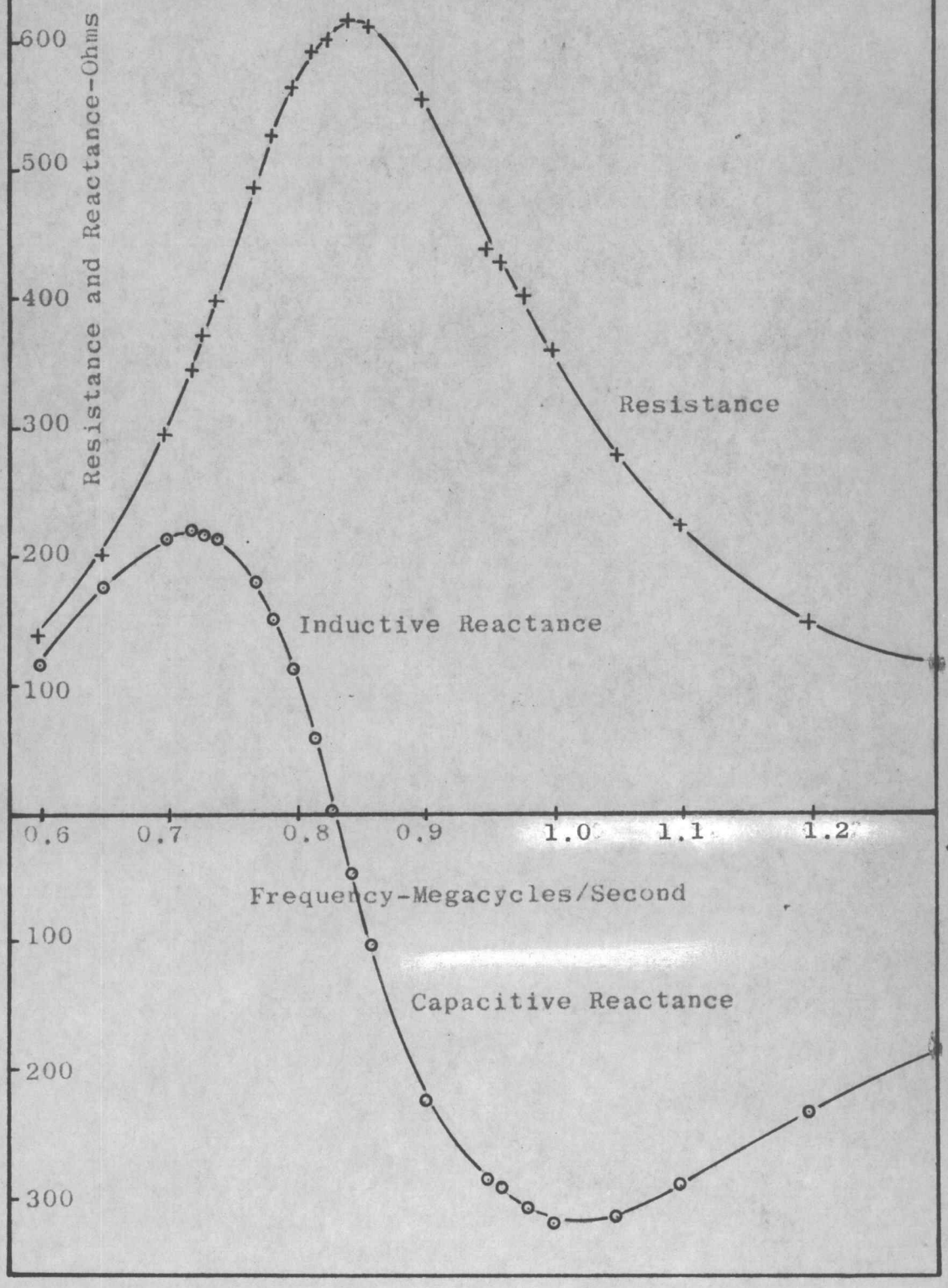

Figure 26

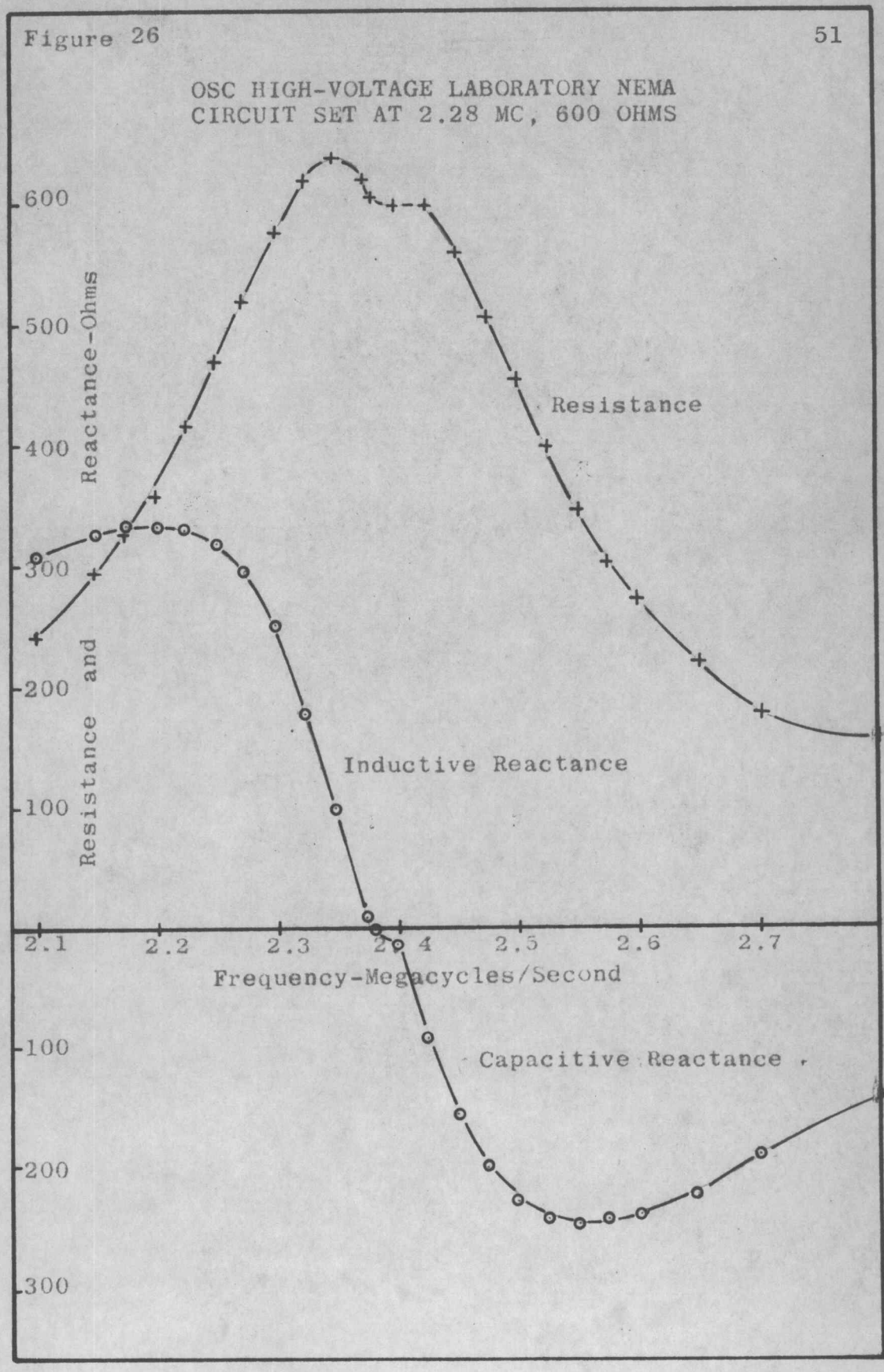
OSC HIGH-VOLTAGE LABORATORY NEMA
CIRCUIT SET AT 2.28 MC, 600 OHMS
Resistance and Reactance-Ohms
600
500
400
300
200
100
Resistance
Inductive Reactance
2.1
2.2
2.3
2.4
2.5
2.6
2.7
Frequency-Megacycles/Second
100
200
300
Capacitive Reactance

Figure 27

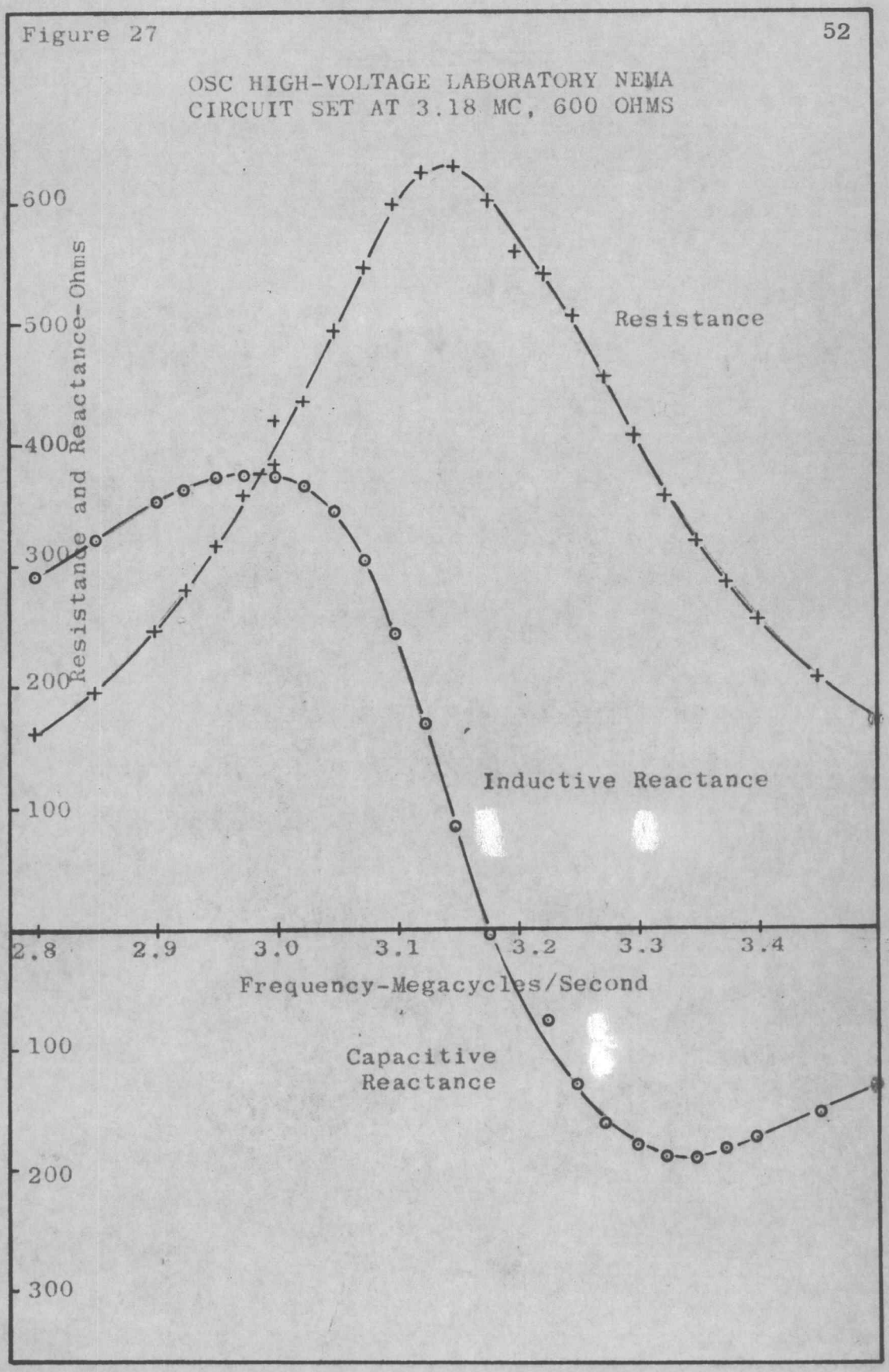
OSC HIGH-VOLTAGE LABORATORY NEMA
CIRCUIT SET AT 3.18 MC, 600 OHMS
Resistance and Reactance-Ohms
600
500
400
300
200
100
Resistance
Inductive Reactance
2.8
2.9
3.0
3.1
3.2
3.3
3.4
Frequency-Megacycles/Second
100
200
300
Capacitive
Reactance

PULSING THE NEMA CIRCUIT WITH A CORONA CURRENT IMPULSE GENERATOR

The Oregon State College NEMA circuit was pulsed by a corona current impulse generator to determine if the conducted radio noise was altered by the circuit. This was done by measuring the radio noise characteristics of the corona generator being used to pulse the NEMA circuit and comparing them with the conducted radio noise measured at the output of the NEMA circuit.

Radio noise characteristics for the corona generator were recorded independently at the four frequencies (0.71, 0.83, 2.28, 3.18 mc) for which the NEMA circuit was tuned and at 0.83 mc with five different resistors (75, 150, 300, 600, 1000 ohms) in the point circuit. Table I contains the tabulated radio noise characteristics for the negative-point corona generator.

The corona generator was placed in the laboratory test area and the NEMA circuit was connected to the point circuit. This was done by removing the point circuit resistors and connecting a lead from the point holder to a two-inch conductor running from the coupling capacitor to the insulator pedestal. The negative terminal of the power supply and the NEMA circuit were grounded at a common point.

The Stoddart meter and the oscilloscope were located in a shielded cage to measure the output of the NEMA circuit. A shielded conductor was run from the power supply to the oscilloscope so that the power supply switch would trigger the oscilloscope trace. This made it possible to record the conducted radio noise characteristics of the NEMA circuit in the same manner the radio noise measurements were made on the corona generator.

The oscillograms in figure 16 show the conducted radio noise characteristics of the NEMA circuit. A comparison of the oscillograms in figures 15 and 16 shows that the NEMA circuit did not alter the conducted radio noise. The tabulated input-output radio noise characteristics of the circuit are found in Table I.

Figures 28-a and b are photographs of the output voltage of the NEMA circuit for two values of terminating resistance with a constant pulse repetition frequency at the input. The circuit is overdamped for both resistance terminations. The oscillograms of input-output radio noise characteristics did not show any effect from the overdamped oscillation of the circuit.

(a)

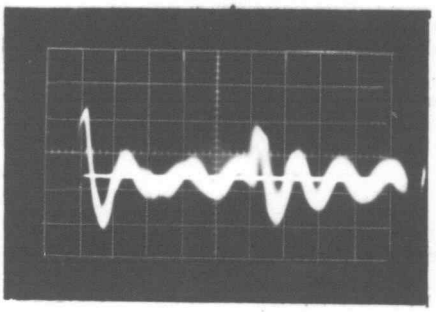

Figure 20. The output voltage of the NEMA circuit while it was being pulsed by a negative point-to-plane corona generator. The NEMA circuit was terminated with a 75-ohm resistor in oscillograph (a) and 1000-ohm resistor in oscillograph (b).

(b)

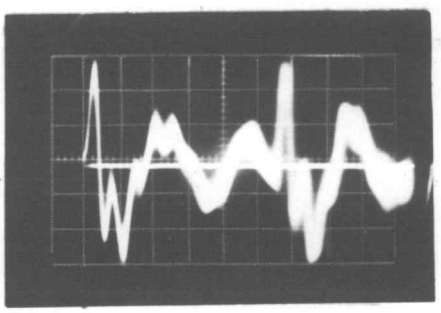

CONCLUSIONS

1. The measurement of radio noise characteristics for positive point-to-plane corona was limited to voltages near onset because of the voluntary flashover of the corona generator.
2. A positive point on tube-to-plane gap configuration will generate current pulses from 2.0 to 10.0 kilopulses per second.
3. The measurement of negative point radio noise was made over wide point-to-plane voltage changes because of the inherent stability of the corona generator.
4. Particular gap configuration of the negative point corona generator will generate current pulses from 0.05 to 1.0 megapulses per second.
5. Negative point corona radio noise indications will occur at finite frequencies, depending upon the pulse repetition frequency.
6. The National Electrical Manufacturers Association circuit for measuring radio noise did not alter the conducted radio noise supplied by a corona current impulse generator.
7. The magnitude of radio noise measured across the resistive termination of the NEMA circuit was directly proportional to the value of the resistor.

BIBLIOGRAPHY

1. Loeb, Leonard B. Fundamental processes of electrical discharge in gases. New York, Wiley, 1939. 717 p.

2. Loeb, Leonard B. Recent developments in analysis of the mechanisms of positive and negative coronas. Journal of Applied Physics 19:882-896. Oct. 1948.

3. National Electrical Manufacturing Association. Methods of measuring radio noise. New York, 1940. 15 p.

4. Stoddart Aircraft Company. Instruction book for radio interference-field intensity meter (NM-20B). Hollywood, Calif., June 1953. 54 p.

5. Trichel, G. W. The mechanisms of the negative point-to-plane corona near onset. Physical Review 54:1078-1084. Dec. 1938.

6. Trichel, G. W. The mechanism of positive point-to-plane corona in air at atmospheric pressure. Physical Review 55:382-390. Feb. 1939.

APPENDIX

APPENDIX I

Linfield Research Institute uses an electrochemical etching process for manufacturing very sharp points from tungsten.

The process requires a one-normal solution of sodium hydroxide, a small piece of nickel, zero to seventy volt alternating-current supply, and the piece of tungsten wire that is to be pointed.

The point is made in this manner: Insert the nickel into the NaOH solution as one electrode connected to one side of the supply. Connect the tungsten to the other supply terminal and into the solution proportional to the length of the conical point desired. Turn the supply up to twelve volts and the chemical reaction commences. Retrieve the point when it has achieved the desired shape. This process will result in pointed or rounded conicals, depending on the length of time the point has been in the process. If a hemispherical-shaped point is desired, insert the tungsten wire into the solution about one-half inch. Allow the process to work until the portion of wire in solution becomes the desired diameter. Then grind off the first eighth inch of the reduced diameter wire. Turn the supply voltage up to seventy volts and hold the point just touching the surface of the liquid. A small

arcing process will take place, after which the point must be checked periodically under a microscope for results.